

Pliocene–Pleistocene sedimentary–tectonic development of the Mesaoria (Mesarya) Basin in an incipient, diachronous collisional setting: facies evidence from the north of Cyprus

ROMESH N. PALAMAKUMBURA* & ALASTAIR H. F. ROBERTSON

University of Edinburgh, School of GeoSciences, Grant Institute, The King's Buildings, James Hutton Road, Edinburgh, UK EH9 3FE

(Received 13 January 2016; accepted 1 November 2016; first published online 21 December 2016)

Abstract – The Mesaoria (Mesarya) Basin exemplifies multi-stage basin development within a regional setting of diachronous continental collision. The Plio-Pleistocene represented a period of major sediment accumulation between two topographic highs, the Kyrenia Range in the north and the Troodos Massif in the south. During Pliocene time, open-marine marls and chalks of the Nicosia (Lefkoşa) Formation accumulated in a shelf setting. The Early Pleistocene period was characterized by a relative fall in sea level and a change to shallower-water bioclastic deposition of the Athalassa (Gürpınar) Formation. The northern margin of the basin was approximately delineated by the E–W neotectonic Ovgos (Dar Dere) fault zone. A carbonate ramp system formed directly to the south of this structural feature. During Early Pleistocene time, the basin evolved from an open-marine shelf to semi-enclosed lagoons with deltaic deposits, and finally to a non-marine aeolian setting, flanked by the rising Kyrenia Range to the north. Synthesis of geological evidence from the Mesaoria (Mesarya) Basin as a whole, including outcrop and borehole evidence from the south, adjacent to the Troodos Massif, indicates that the Pliocene – Early Pleistocene represented a relatively quiescent period. This intervened between Late Miocene – earliest Pleistocene southward thrusting–folding of the Kyrenia Range and Pleistocene intense surface uplift of both the Kyrenia Range and the Troodos Massif. The basin development reflects flexurally controlled collapse during Late Miocene – earliest Pliocene time related to southward thrusting, followed by strike-slip during westward tectonic escape of Anatolia, and finally regional uplift controlled by under-thrusting of continental crust from the south, as collision progressed.

Keywords: Northern Cyprus, sedimentology, Neogene, foredeep basin.

1. Introduction

The main aim of this paper is to describe and interpret the Pliocene–Pleistocene sedimentary development of the northern part of the intermontane Mesaoria (Mesarya) Basin (Fig. 1). The southern part of the Mesaoria (Mesarya) Basin has been the focus of several previous studies (Ducloz, 1965; McCallum & Robertson, 1990, 1995a,b; Schirmer *et al.* 2010; Kinnaird, Robertson & Morris, 2011; Weber *et al.* 2011). In contrast, little work has been carried out on the Pliocene and Pleistocene deposits exposed in the northern part of the Mesaoria (Mesarya) Basin, and those associated with the Kyrenia Range to the north. Here, we present new facies-based evidence from the northern part of the Mesaoria (Mesarya) Basin, which we combine with comparable information from its southern part to allow the first overall synthesis of the Pliocene – Early Pleistocene tectonic–sedimentary development of this basin in its regional tectonic setting.

The Mesaoria (Mesarya) Basin represents an excellent opportunity to study facies and depositional processes within a tectonically active sedimentary basin, which was influenced by rising landmasses to the north and the south, within a regional collisional setting. The northern margin of the basin was bounded by the Kyrenia Range lineament, and the southern margin by the Troodos Massif (Fig. 1).

The collision of the Eratosthenes Seamount (Fig. 1) with the Cyprus Trench to the south of Cyprus is inferred to have been a major tectonic control of the surface uplift of the Troodos Massif during Pleistocene time, within a regional setting of incipient continental collision of the African and Eurasian plates (Robertson, 1977, 1990, 1998; Robertson & Dixon, 1984; Poole, Shimmield & Robertson, 1990; Poole & Robertson, 1998; Kempler, 1998; Kinnaird, Robertson & Morris, 2011; Kinnaird & Robertson, 2013). Recently, it has been inferred that the collision also affected the Kyrenia Range further north (Palamakumbura *et al.* 2016b). Other tectonic models have postulated late-stage continental collisional setting (Calon, Aksu & Hall, 2005), regional strike-slip/transpression

* Author for correspondence: rpalamakumbura@gmail.com

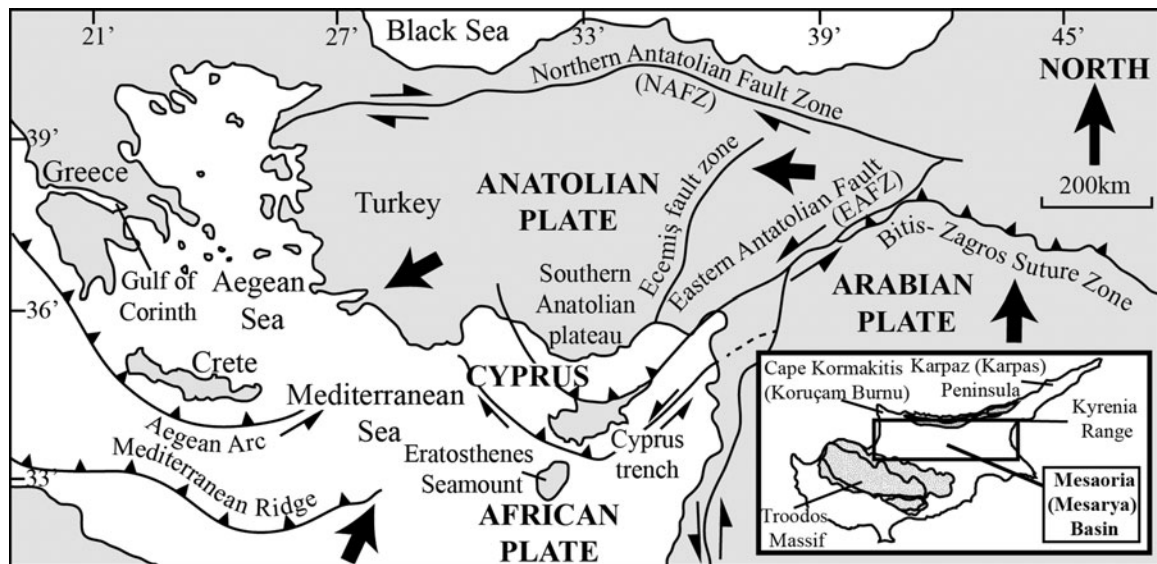


Figure 1. Summary tectonic map of the Eastern Mediterranean during Pleistocene time (modified from McCay *et al.* 2013).

(Harrison *et al.* 2004) or slab break-off during late-stage subduction (Schildgen *et al.* 2012). Here, we relate the Mesaoria (Mesarya) Basin to a setting of incipient and diachronous continental collision, in which the successive stages of Pliocene and Pleistocene basin development represent the sequential influences of thrust loading, strike-slip and regional uplift.

Prior to Pliocene time, the area of the Mesaoria (Mesarya) Basin formed part of an open-marine depositional system, bordering the Anatolian continent to the north (McCay & Robertson, 2012). During Late Miocene – earliest Pliocene times the Mesaoria (Mesarya) Basin developed into a flexurally controlled foreland basin that was initiated by southward overthrusting of the Kyrenia Range. Prior to this time the lineament formed part of the former northerly, active continental margin of the Southern Neotethys ocean (Robertson, Parlak & Ustaömer, 2012; Robertson *et al.* 2013). During the subsequent Pliocene–Pleistocene period, which is the main subject of this paper, the Mesaoria (Mesarya) Basin developed differently from the pattern of a subsiding foreland basin (Beaumont, 1981; Stockmal & Beaumont, 1987). During Pliocene time, the evidence from the northern part of the basin, discussed in detail here, indicates sedimentation in a relatively quiescent basin that was influenced by regional sinistral strike-slip. The Mesaoria (Mesarya) Basin then underwent uplift during Early Pleistocene time, represented by a shallowing marine sequence, as documented here. The uplift culminated in a marine regression and the emergence of the present Kyrenia mountain range during Mid-Late Pleistocene time in a setting of incipient continental collision (Palamakumbura *et al.* 2016b; Palamakumbura & Robertson, 2016).

2. Methodology

The fieldwork focused on the northern part of the Mesaoria (Mesarya) Plain, the Karpaz (Karpas)

Peninsula to the northeast and the Koruçam Burnu (Cape Kormakiti) area in the northwest, where most of the Pliocene and Pleistocene deposits are located (Fig. 1). Building on regional geological mapping (e.g. Constantinou, 1995) and previous studies, mainly by Baroz (1979), we have carried out a sedimentological study, mainly through sedimentary logging and facies analysis, to determine the palaeoenvironments represented and how they changed through time. We describe and interpret the different sedimentary facies, termed A1–A2 for open-marine sediments, B1–B4 for shallow-marine sediments, C1–C2 for deltaic sediments, D1–D3 for lagoonal sediments and E1–E2 for aeolian sediments. The sedimentary results are then integrated into the regional tectonic setting to help interpret the basin development.

For the stratigraphy, we utilize the long-standing Greek-based nomenclature, with more recently introduced Turkish equivalents in parentheses. For geographical localities we mostly use recently introduced Turkish names, with traditional names (mostly Greek) in parentheses.

3. Geological framework of northern Cyprus

The sedimentary development of the northern part of the Mesaoria (Mesarya) Basin is intimately linked to the Kyrenia Range to the north. The geological record of the Kyrenia Range spans Late Palaeozoic to Recent time (Ducloz, 1972; Baroz, 1979; Robertson & Woodcock, 1986). The Triassic to Miocene geological history of the range has particular implications for the Pliocene and Pleistocene palaeoenvironmental and depositional settings discussed here. In particular, the developing structures and lithologies of the Kyrenia Range influenced the distribution and composition of the bordering Neogene–Recent sediments. During Triassic time, the Kyrenia Range formed part of a rifted continental fragment that was located between the

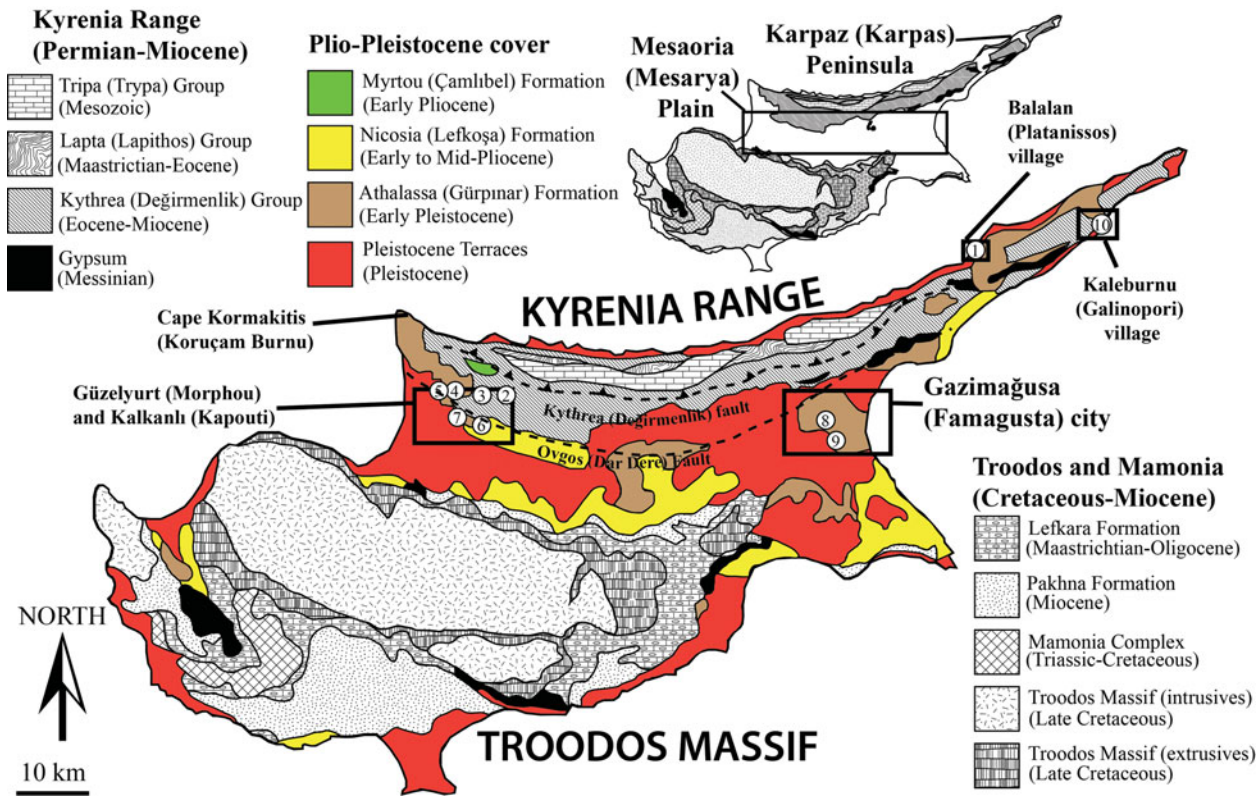


Figure 2. (Colour online) Summary geological map of Cyprus showing the distribution of Pliocene and Pleistocene deposits (modified from Constantinou, 1995) and the location of the logged sections in Figure 5.

North African continent to the south and a regional-scale Tauride microcontinent to the north (Robertson & Woodcock, 1986; Robertson, Parlak & Ustaömer, 2012). During Late Triassic to Cretaceous times the rifted crust was capped by a subsiding carbonate platform, with the accumulation of shallow-marine carbonates (limestones and dolomites), represented by the Trypa (Tripa) Group (Baroz, 1979; Robertson & Woodcock, 1986) (Fig. 2). Today, these competent lithologies dominate the landscape of the central part of the Kyrenia Range and have contributed much detritus to the Mesaoria (Mesarya) Basin during Neogene to Recent time (McCay & Robertson, 2012). In contrast, the Mesozoic platform carbonates are largely absent from both the eastern and western parts of the Kyrenia Range, where Cenozoic volcanic rocks, pelagic carbonates and also Miocene siliciclastic sedimentary rocks are prevalent (Ducloz, 1972; Baroz, 1979; Robertson & Woodcock, 1986). The geological differences along the length of the Kyrenia Range influenced the composition of Neogene sediments within the Mesaoria (Mesarya) Basin.

During Late Cretaceous time, the Mesozoic shallow-water sequence was deeply buried and metamorphosed to greenschist facies (Baroz, 1979; Robertson *et al.* 2013). Soon afterwards, these rocks were exhumed and covered by pelagic limestones and basic volcanic rocks during latest Cretaceous to Eocene time, as represented by the Lapithos (Lapta) Group (Fig. 2). During Middle Eocene time, siliciclastic sediments and large-scale debris-flows

(olistostromes) were laid down (uppermost part of the Lapithos (Lapta) Group), followed by a major phase of southward thrusting (Baroz, 1979; Robertson *et al.* 2013; Robertson & Kinnaird, 2016). From Late Eocene to Late Miocene times, the thrust belt was covered by mostly deep-marine, siliciclastic gravity-flow deposits of the Kythrea (Değirmenlik) Group (Weiler, 1970; McCay & Robertson, 2012, 2013). These sediments form the ‘basement’ of the Pliocene–Pleistocene-aged sediments of the northern part of the Mesaoria (Mesarya) Basin, where exposed within the study area.

The Messinian salinity crisis resulted in the precipitation of gypsum and related deposits in small tectonically controlled basins to the south of the Kyrenia Range (Necdet & Anıl, 2006; McCay *et al.* 2013). During Late Miocene to earliest Pliocene times, straddling the Messinian salinity crisis, the Kyrenia Range underwent a second phase of major southward thrusting. Structural evidence indicates that this deformation took place within a sinistral transpressive stress regime (McCay & Robertson, 2013; Robertson & Kinnaird, 2016). Adjacent to the Kyrenia Range, the Pliocene period was characterized by the accumulation of mostly fine-grained, argillaceous sediments in a shelf setting, represented by the Nicosia (Lefkoşa) Formation. This was followed during Pleistocene time by the deposition of shallow-water, bioclastic carbonates of the Athalassa (Gürpınar) Formation (Baroz, 1979; McCay & Robertson 2012, 2013). Rapid emergence to form the present Kyrenia Range took place

Kyrenia Range Stratigraphy					
Time				Stratigraphy	
System	Series	Subseries	Italian marine stages	Group	Formation
Quaternary	Holocene		Tarranlian	Fanglomerate Group (K0-K5 terraces)	
	Pleistocene	Late			
		Middle	Ionian		
		Early	Calabrian		
	Emilian				
			Santernian		
Neogene	Pliocene	Late	Piacenzian	Mesaoria (Mesarya)	Athalassa (Gürpınar)
					Early

Figure 3. Stratigraphy of the Pliocene and Pleistocene deposits of northern Cyprus according to different authors (Ducloz, 1972; Baroz, 1979; Hakyemez *et al.* 2000; McCay *et al.* 2013, and this study).

during Middle to Late Pleistocene times (Ducloz, 1972; Baroz, 1979; Robertson & Woodcock, 1986), as recently elucidated by a combination of palaeomagnetic, uranium disequilibria dating of solitary coral and optically stimulated luminescence analysis (Palamakumbura *et al.* 2016a,b).

4. Stratigraphy of the Mesaoria (Mesarya) Basin

The stratigraphy of the Pliocene and Pleistocene deposits of the Mesaoria (Mesarya) Basin was established by Ducloz (1965) (see Fig. 3), with proposed modifications by Baroz (1979), McCallum & Robertson (1995b) and Harrison *et al.* (2004). In the north of Cyprus, the Pliocene to Pleistocene deposits are represented by the Mesaoria (Mesarya) Group, which includes the Myrtou (Çamlıbel), Nicosia (Lefkoşa) and Athalassa (Gürpınar) Formations and the Fanglomerate Group (Ducloz, 1972; Baroz, 1979; Robertson & Woodcock, 1986; McCay *et al.* 2013; Fig. 3). The Pliocene period began with the localized deposition of mostly marls of the Myrtou (Çamlıbel) Formation, which have been locally dated using strontium isotopes as Early Pliocene in age (McCay *et al.* 2013). Deposits of the Myrtou (Çamlıbel) Formation are overlain by the more widespread marls and chalks of the Nicosia (Lefkoşa) Formation (Henson, Browne & McGinty, 1949; Baroz, 1979). Conformably above come calcarenites, marls and conglomerates, which constitute the Athalassa (Gürpınar) Formation, of Middle Pliocene to Early Pleistocene age (Henson, Browne & McGinty, 1949; Baroz, 1979; Palamakumbura *et al.* 2016b).

The Athalassa Formation was defined as lying stratigraphically above the Nicosia (Lefkoşa) Formation (Ducloz, 1965; Baroz, 1979; McCallum & Robertson,

1990, 1995a; Kinnaird, Robertson & Morris, 2011). More recently, based mostly on a detailed study of the Greater Nicosia area, Harrison *et al.* (2004) reduced the Athalassa (Gürpınar) Formation to the status of a member within the Nicosia (Lefkoşa) Formation. This alternative stratigraphy is tested here in the light of new evidence.

The Athalassa (Gürpınar) Formation in the western Mesaoria (Mesarya) Plain is deformed by the E–W-trending Ovgos (Dar Dere) fault zone (Harrison *et al.* 2004; McCay & Robertson, 2013; Fig. 2). The fault zone underwent sinistral strike-slip/transpressional deformation during Late Miocene time, progressing to strike-slip during Late Pliocene – Pleistocene times, based on structural kinematic evidence (e.g. slickensides) along the Ovgos (Dar Dere) fault zone (McCay & Robertson, 2013).

5. Age constraints

The Nicosia (Lefkoşa) Formation in the northern part of the Mesaoria (Mesarya) Basin is dated using biostratigraphy (Baroz, 1979; Hakyemez *et al.* 2000; A. Lord in Harrison *et al.* 2004, 2008). The planktonic foraminifera *Globorotalia margaritae* and *Globorotalia acostaensis* in chalks within the Nicosia (Lefkoşa) Formation represent the Pliocene zones N19 to N20 (Baroz, 1979; Hakyemez *et al.* 2000; A. Lord in Harrison *et al.* 2008).

The age of the Athalassa (Gürpınar) Formation in the northern Mesaoria Basin and the Kyrenia Range remains poorly constrained, although equivalent facies in the southern part of the basin are better dated as Early Pleistocene. The recently changed age of the Pliocene–Pleistocene boundary from 1.6 Ma to 2.6 Ma (Cohen & Gibbard, 2010), in practice means that deposits that

were previously classified as Late Pliocene are now assigned to the Early Pleistocene. Foraminifera that are characteristic of the Pliocene are absent from the Athalassa (Gürpınar) Formation (excluding reworked tests; see below) (Baroz, 1979; Hakyemez *et al.* 2000; A. Lord *in* Harrison *et al.* 2008). Palaeomagnetic analysis of the Athalassa (Gürpınar) Formation in the north of the Mesaoria (Mesarya) Plain has revealed the existence of reversed polarities, indicating deposition prior to the most recent palaeomagnetic reversal at 0.78 Ma (Palamakumbura *et al.* 2016b). The available evidence suggests an Early Pleistocene age for the Athalassa (Gürpınar) Formation within the northern part of the Mesaoria (Mesarya) Basin, similar to the age of the better-dated exposures further south.

6. Distribution of the Nicosia (Lefkoşa) and Athalassa (Gürpınar) formations

The Nicosia (Lefkoşa) Formation is widely exposed in the western part of the Mesaoria (Mesarya) Plain and in the Karpaz (Karpas) Peninsula (Fig. 2). The Athalassa (Gürpınar) Formation is exposed most extensively in the western and eastern parts of the Mesaoria (Mesarya) Plain, around Koruçam Burnu (Cape Kormakiti) and in the Karpaz (Karpas) Peninsula (Fig. 2). The exposed thickness of the Nicosia (Lefkoşa) Formation in these areas ranges from 5 m to nearly 16 m. In contrast, beneath the southern part of the Mesaoria Plain the Nicosia (Lefkoşa) Formation reaches *c.* 900 m in thickness, based on water-well and borehole data (McCallum & Robertson, 1990; Harrison *et al.* 2008).

The Athalassa (Gürpınar) Formation is best exposed within the central northern part of the Mesaoria (Mesarya) Plain and in the low-lying western and eastern extremities of the Kyrenia Range (Fig. 2). In the western part of the Mesaoria (Mesarya) Plain the formation is preserved in a series of isolated terraces, which expose deposits up to 10 m thick. The Athalassa (Gürpınar) Formation in the Karpaz (Karpas) Peninsula and the Burnu Koruçam (Cape Kormakiti) Peninsula (Fig. 2) extends almost continuously from the northern to the southern coasts, comprising deposits that are 6 to 40 m thick (Fig. 2). In addition, the Nicosia (Lefkoşa) Formation is well exposed in the Karpaz (Karpas) Peninsula, where it comprises open-marine chalks and marls that are conformably overlain by diverse shallow-marine facies of the Athalassa (Gürpınar) Formation. The contact between the two formations, as exposed in the Karpaz (Karpas) Peninsula, is interpreted as a relatively abrupt shallowing-upward event.

7. Facies of the Nicosia (Lefkoşa) Formation

The Pliocene facies of the Nicosia (Lefkoşa) Formation provide evidence for the early development of the basin. The Mesaoria (Mesarya) Basin, as defined here, began with the deposition of transgressive Plio-

cene sediments that post-dated the Messinian salinity crisis and southward thrusting of the Kyrenia Range lineament.

The Nicosia (Lefkoşa) Formation in the outcrops studied is represented by two different facies: first, planar-bedded chalks and, secondly marls (see Table 1; facies A1 and A2). Chalk beds range from 20 cm to *c.* 1 m thick and are well-lithified. In contrast, marl beds are <30 cm thick and poorly lithified. The chalk (A1 facies) and marl (A2 facies) are interbedded and laterally continuous on an outcrop scale.

The A1 facies contains abundant planktonic foraminifera in a micritic matrix. In contrast, the A2 facies includes only minor planktonic foraminifera within a calcareous and argillaceous matrix. The planktonic foraminifera in both the chalk and marl deposits are mostly well preserved and appear to be *in situ*, ranging from up to 90% of the chalk (by volume), compared to *c.* 10% of the marl. Globigerinidae predominate (Fig. 4a–c), together with subordinate Nodosariidae and Rotaliidae and representatives of several other families (Fig. 4d–f).

The presence of a predominantly planktonic biota indicates an undifferentiated open-marine environment within the Mesaoria (Mesarya) Basin and the Karpaz (Karpas) Peninsula.

8. Facies of the Athalassa (Gürpınar) Formation

The facies that are represented in the outcrops of the Athalassa (Gürpınar) Formation range from shallow-marine (neritic), to paralic (transitional), to non-marine (Table 1).

8.a. Shallow-marine facies

Shallow-marine facies dominate the Athalassa (Gürpınar) Formation (Fig. 5), comprising the B1 to B4 facies (Table 1). The B1 facies range from 1 to 16 m thick (Fig. 5, logs 5 to 10), as exposed in the central parts of the Mesaoria (Mesarya) Plain and along the southern coast of the Karpaz (Karpas) Peninsula (Fig. 2).

The B1 facies is composed of medium-grained, planar-bedded grainstone, in beds typically *c.* 1 m thick. Benthic foraminifera dominate the biota, together with minor amounts of planktonic foraminifera. The B1 grainstone facies also contains minor amounts of fine- to medium-grained lithic material. In addition, scoured, lenticular structures (50 cm wide by 1 m long) occur in the eastern part of the Mesaoria (Mesarya) Plain (Fig. 5, log 8; Fig. 6a). These channel-like features are infilled with structureless, medium-grained grainstone. At several localities, the B1 facies is interbedded with well-lithified marl (Fig. 5, logs 8 and 9). Blocks of lithified sandstone and marl are preserved along erosional surfaces (10–20 cm in size) within the grainstones (Fig. 5, log 10; Fig. 6b).

In the western part of the Mesaoria (Mesarya) Plain (Fig. 3, logs 6 and 7), well-exposed packages of gently

Table 1. Summary facies descriptions of the Nicosia (Lefkoşa) and Athalassa (Gürpınar) Formations in the northern part of Cyprus

	Facies code	Facies	Description	Depositional environment
Open-marine facies	A1	Chalk	Fine-grained deposit dominated by planktonic foraminifera, set in micrite.	Low-energy nutrient-rich hemipelagic environment.
	A2	Marl	Fine-grained mudstone with poorly preserved planktonic foraminifera.	Low-energy nutrient-poor hemipelagic environment.
Shallow-marine facies	B1	Thick-bedded grainstone	Grainstone comprising dominantly benthic foraminifera, bioclastic and lithogenous grains. Sedimentary structures include <i>c.</i> 1 m-thick parallel bedding.	Open-marine basin.
	B2	Thick-bedded rudstone	Rudstone dominantly comprising calcareous red algae, bioclastic and lithogenous grains. Sedimentary structures include centimetre-thick bedding.	Inner to mid-carbonate ramp.
	B3	Bedded packstone	Packstone comprised of carbonate and clastic material. Sedimentary structures include centimetre-scale bedding.	Inner to mid-carbonate ramp.
	B4	Low-angle trough cross-bedded grainstone	Grainstone comprising carbonate, bioclastic and lithogenous grains. Sedimentary structures include cross-bedding with foresets <30°.	Inner to mid-carbonate ramp.
Deltaic facies	C1	Bioclastic conglomerate	Conglomerate with poorly sorted clasts of locally sourced bioclastic and lithogenous material and large bivalve shells.	Local reworking by high-energy flows in a shallow-marine environment, incorporating carbonate and lithic debris.
	C2	Fluvial conglomerate	Well-rounded to sub-angular clasts within matrix-supported conglomerate. Clast composition varies, depending on local geology. The matrix is grainstone. Occasional bored clasts of metacarbonate are present.	Fluvial drainage system.
Lagoonal facies	D1	Thin-bedded grainstone	Grainstone comprised of carbonate, bioclastic and lithogenous grains. Sedimentary structures include centimetre-scale bedding.	Low-energy coastal lagoons.
	D2	Oyster floatstone	Decalcified monospecific oysters occur within fine-grained grainstone.	Low-energy lagoonal environment. Single species of bivalve suggests stressed environment.
	D3	Oncoid floatstone (Oncolite)	Grainstone with well-preserved oncolites.	Inter-tidal to sub-tidal shallow-marine environment.
Aeolian facies	E1	High-angle planar cross-bedded grainstone	Grainstone comprising carbonate and clastic grains. Sedimentary structures include <i>c.</i> 2 m thick cross-bedded units with a foreset dip of between 30° and 45°.	Dune deposits reflect an E–W palaeowind system sub-parallel to the Kyrenia Range.
	E2	Breccia	Poorly sorted breccia composed of reworked clasts of aeolian grainstone.	Erosion within a non-marine environment.

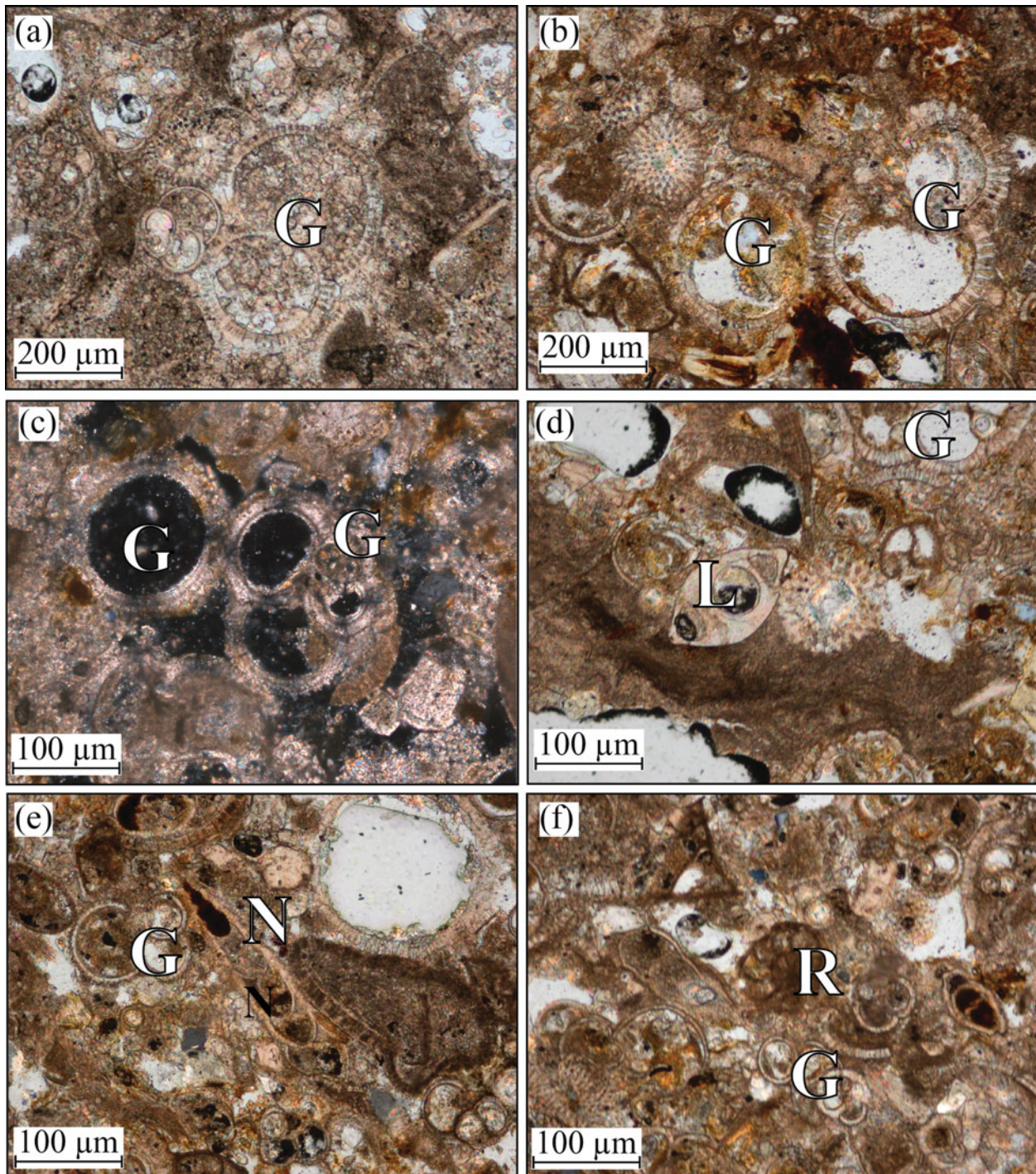


Figure 4. (Colour online) Photomicrographs of planktonic foraminifera from interbedded marls and chalks within the Nicosia (Lefkoşa) Formation: (a) Globigerinidae [G]; (b) Globigerinidae [G]; (c) Globigerinidae [G]; (d) *Lenticulina* [L] (benthic foraminifera) and Globigerinidae [G]; (e) Globigerinidae [G] and Nodosariidae [N]; and (f) Rotaliidae [R] and Globigerinidae [G].

southward-dipping strata (*c.* 100 m long by *c.* 10 m thick) are interpreted as clinoforms (Fig. 7). The measured dips of these features range from *c.* 30° in the north, to < 10° in the south, away from the Ovgos (Dar Dere) fault zone. The clinoforms are dominated by the B1 grainstone facies. These key structures are discussed in more detail later in the paper. In some beds, *Thalassinoides* (an ichnofacies) (Fig. 5, logs 8 and 10) is well developed, as exposed on some vertical rock faces (Fig. 6c, d) and bedding planes (Fig. 6e). Bi-

valves (e.g. *Ostrea* sp.; Fig. 6f) are abundant along several horizons. In addition, beds rich in gastropod casts (i.e. Turritellidae; Fig. 6g) and bivalve casts (Fig. 5, log 8) occur locally.

The B2 facies (Table 1) is only exposed along the western extension of the Ovgos (Dar Dere) fault zone, where it directly overlies the B1 grainstone facies and locally forms the mid part of the Athalassa (Gürpınar) Formation (Fig. 5, log 6). The B2 facies is dominated by calcareous red algae, including

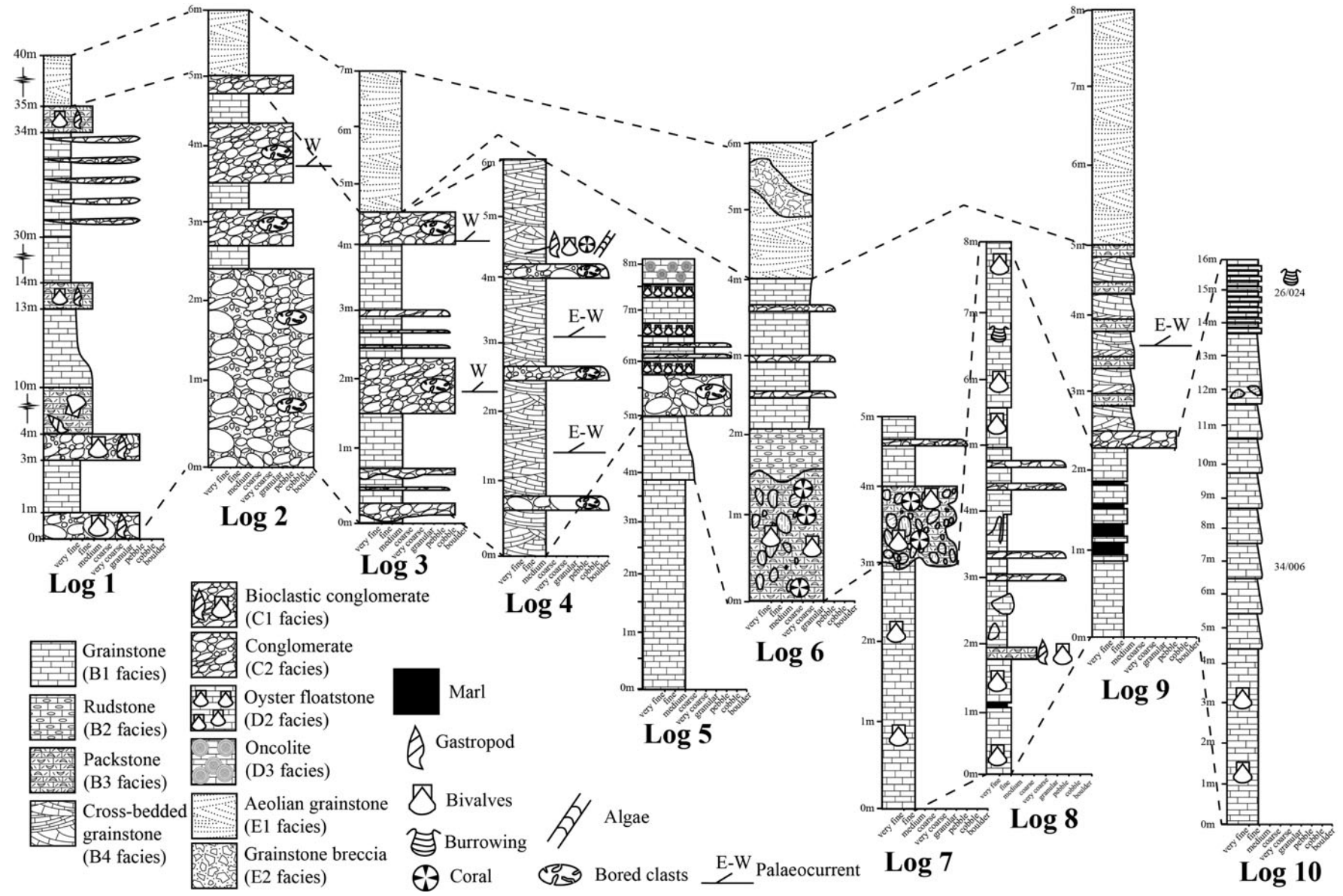


Figure 5. Sedimentary logs of the Athalassa (Gürpınar) Formation that were measured during this study (see Fig. 2 for locations). Facies-based correlations are shown by dashed lines.

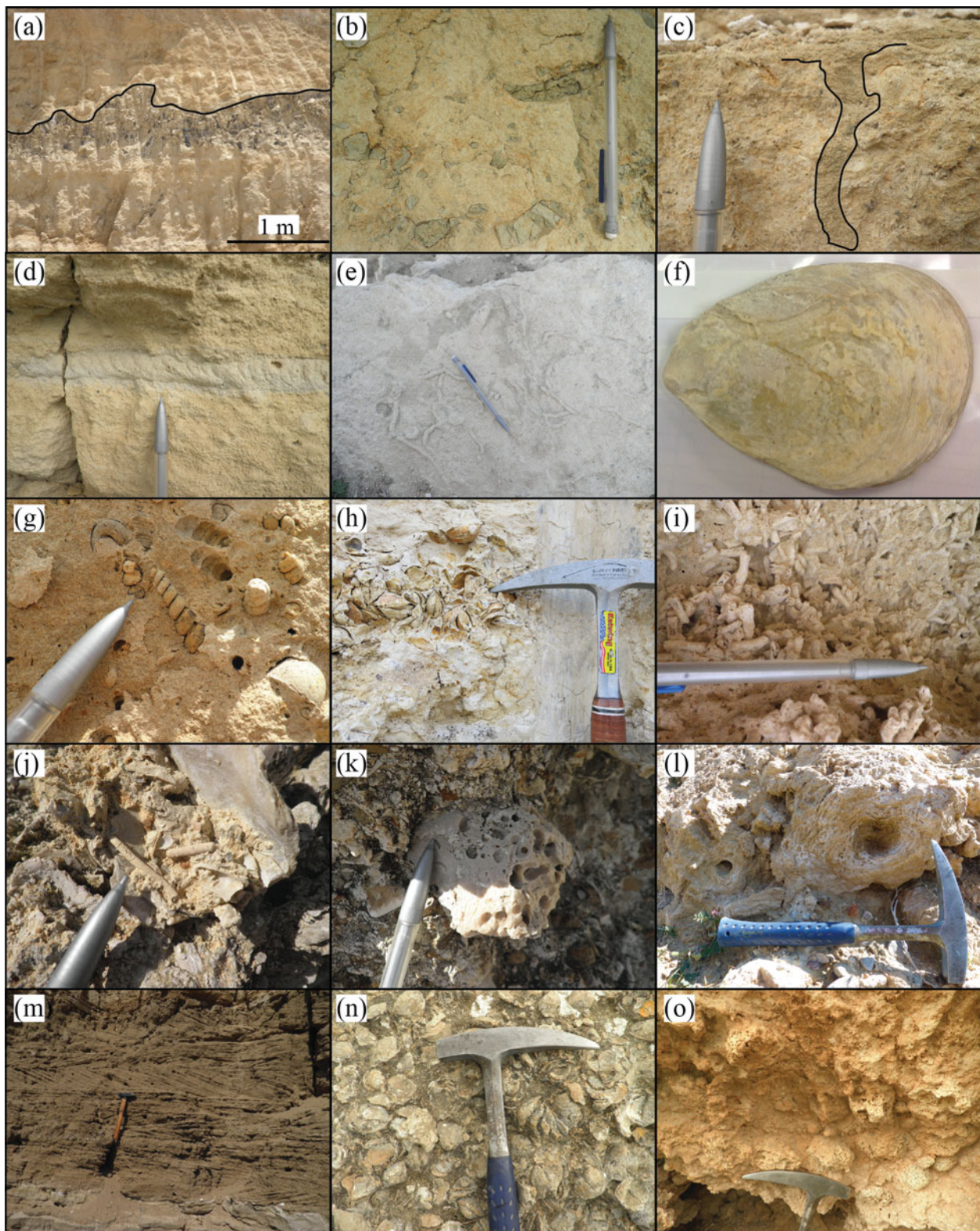


Figure 6. (Colour online) Photographs of key field features of the Athalassa (Gürpınar) Formation: (a) erosional surface within the B1 grainstone; (b) reworked clasts of marl within the B1 grainstone; (c, d) vertical section through *Thalassinoides* ichnofacies within the B1 grainstone; (e) *Thalassinoides* on a horizontal bedding surface; (f) *Ostrea* bivalve shell (c. 10 cm long); (g) casts of the gastropod Turritellidae; (h) casts of bivalves; (i) *Cladocora* coral; (j) bryozoan-rich deposit; (k) bored clast; (l) algae; (m) low-angle cross-bedding; (n) *Ostrea*-rich floatstone; and (o) oncolite-rich floatstone (oncolite). Pencil length for scale is c. 15 cm; hammer head length is c. 30 cm.

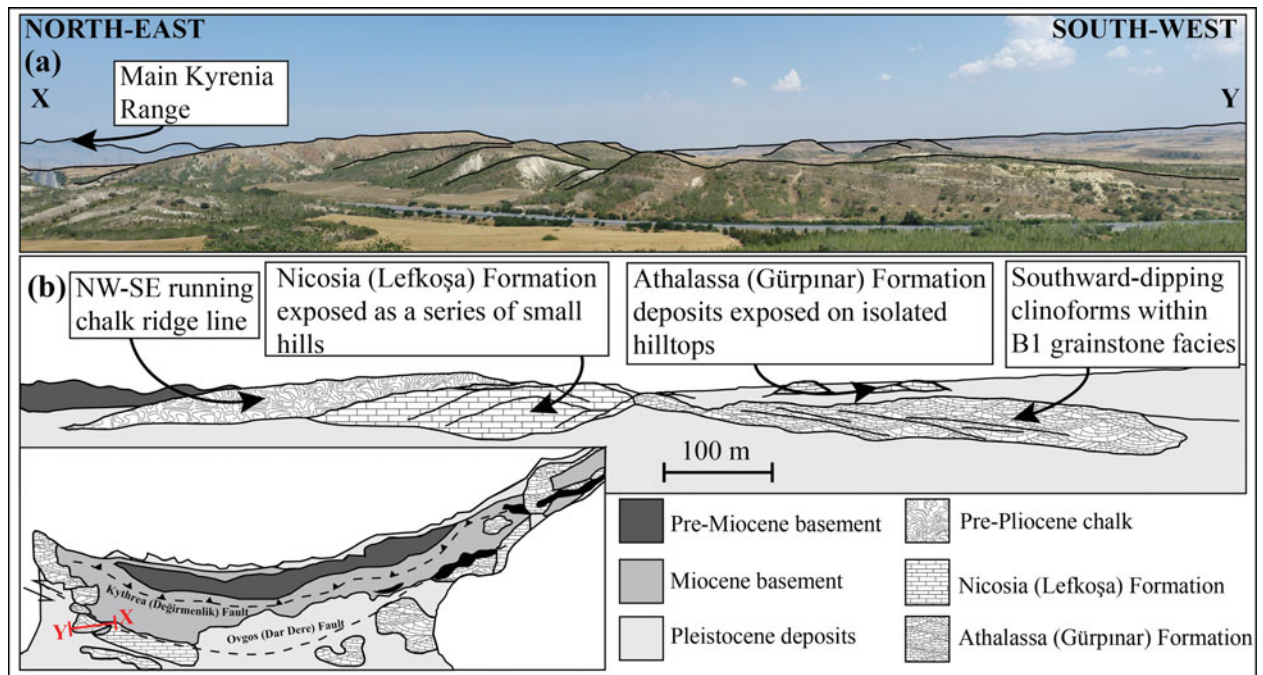


Figure 7. (Colour online) Overview of the clinoform system within the B1 facies grainstone on the northeastern part of the Mesaoria (Mesarya) Basin, directly south of the Ovgos (Dar Dere) fault zone.

Lithophyllum and *Lithothamnion*, together with minor amounts of reworked biogenic material, including benthic foraminifera and bivalve fragments. Quartz, chert and serpentinite are present as associated lithic material.

The B3 facies is exposed throughout the Mesaoria (Mesarya) Plain, where it is interbedded with the B1 facies grainstone, within the mid and upper parts of the succession (Fig. 5, logs 1, 8 and 9). The B3 packstone facies (Table 1) comprises 10 to 30 cm-thick beds, with variable proportions of bivalves, gastropods, solitary corals and bryozoans (Fig. 6h–l). The biogenic material is little altered but variably fragmented. Lithic clasts vary in size from 0.5 to 30 cm and range from well-rounded to sub-angular.

The B4 facies, which is mostly composed of medium-grained grainstone, conformably overlies the B1 to B3 facies, where it is exposed in the eastern part of the Mesaoria (Mesarya) Plain (Fig. 5, log 9) and also in the Karpaz (Karpas) Peninsula. The B4 grainstone facies (Table 1) is characterized by low-angle (<30°), planar cross-bedding and sub-horizontal parallel bedding. The individual cross-bedded and planar-bedded units range from 30 to 50 cm thick, within 1 to 3 m thick larger-scale depositional units (Fig. 5, log 9; Fig. 6m). Sparse, palaeocurrent data indicate both easterly and westerly sediment transport in different areas (Fig. 5).

8.a.1 Grainstone and rudstone composition

The B1 grainstone facies are rich in benthic foraminifera, especially *Miliolida* sp. and *Neorotalia* sp. (Fig. 8a, b). Peneroplidae were recorded only in the

Karpaz (Karpas) Peninsula (Fig. 8c). Lesser amounts of the benthic foraminifera *Anomalina* sp., *Textulariidae*, *Rotaliidae*, *Eponides* sp., *Valvulina* sp. and *Elphidium* sp. are also present. In addition, planktonic foraminifera of the same species as those identified within the underlying Nicosia (Lefkoşa) Formation chalks and marls (see Section 7 above) make up a relatively small proportion (<25%) of the foraminifera observed within the grainstones (Fig. 8d–j).

The B1 to B4 facies include large amounts of carbonate and lithoclastic material. Carbonate grains are predominantly calcareous red algae, echinoderms, bivalves, bryozoans and benthic foraminifera (Fig. 9a–c). In places, rudstones are dominated by calcareous red algae, which occur as millimetre-sized fragments, surrounded by fine-grained micritic cement (Fig. 9a). Serpulid worm tubes are commonly preserved, ranging from intact to fragmented (Fig. 9e). Microbial carbonate (algal) (<200 μm thick) commonly encrusts serpulid worm tubes, echinoderm fragments and reworked calcareous algae (Fig. 9f, g). Reworked echinoderm plates commonly have a speckled texture owing to the development of micritic overgrowths (Fig. 9i, j). Ostracods and bryozoans (Fig. 8d) also occur locally in minor amounts.

Reworked clasts form a major constituent of the grainstone deposits and can be divided into two groups: (1) lithic clastic material of extraformational origin, and (2) bioclastic grains of intraformational origin. The lithic material is mostly monocrystalline and polycrystalline quartz (Fig. 9k), chert, serpentinite, diabase, metacarbonate rock and feldspar. The reworked bioclastic material contains benthic and planktonic foraminifera and calcareous red

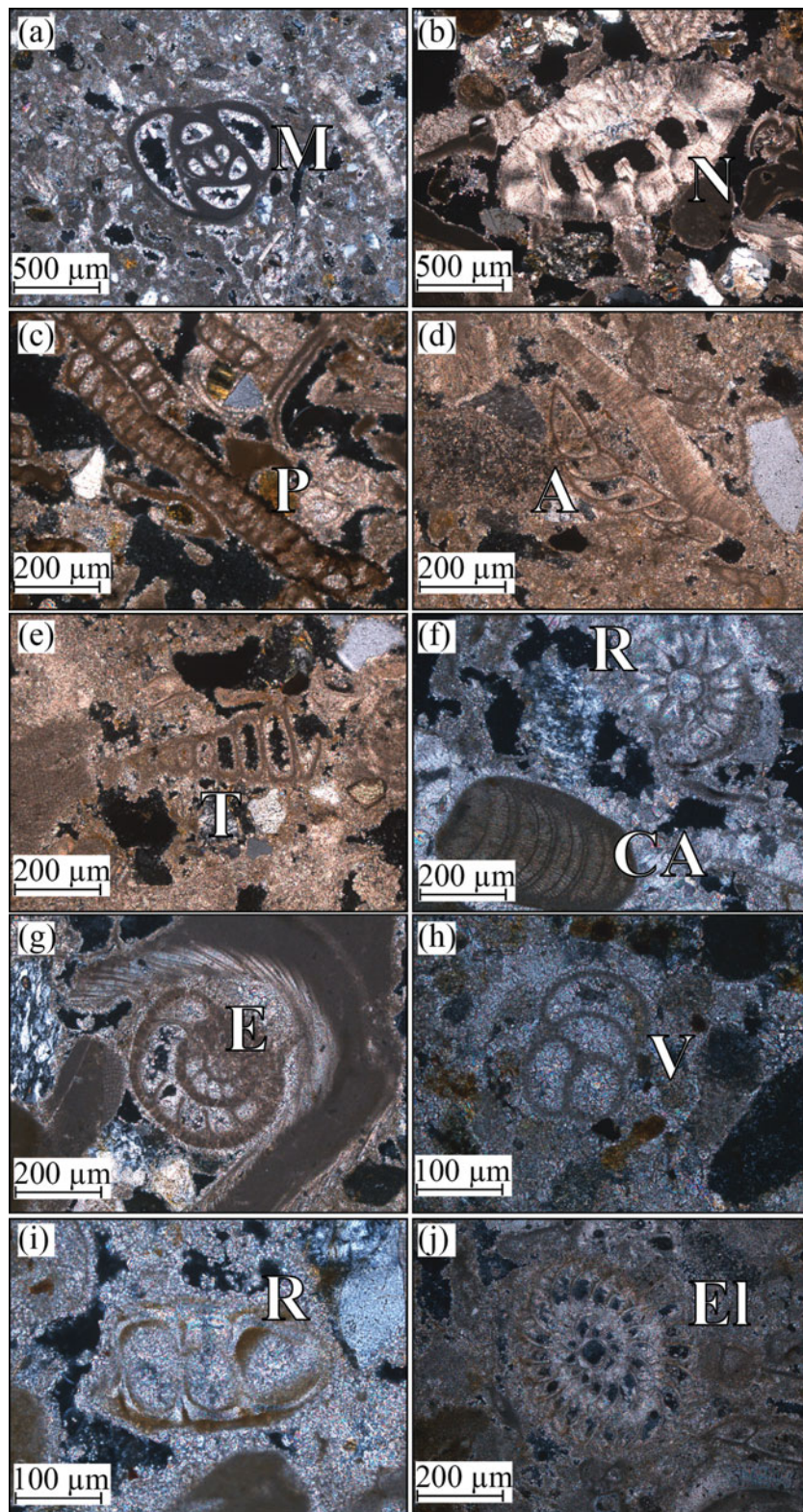


Figure 8. (Colour online) Photomicrographs of benthic foraminifera from the Athalassa (Gürpınar) Formation in the northern Mesaoria (Mesarya) Plain and the Karpaz (Karpas) Peninsula: (a) *Miliolida* [M]; (b) *Neorotalia* [N]; (c) Peneroplidae [P]; (d) *Anomalina* [A]; (e) Textulariidae [T]; (f) Rotaliidae [R] and calcareous red algae [CA]; (g) *Eponides* [E]; (h) *Valvulina* [V]; (i) Rotaliidae [R]; and (j) *Elphidium* [E].

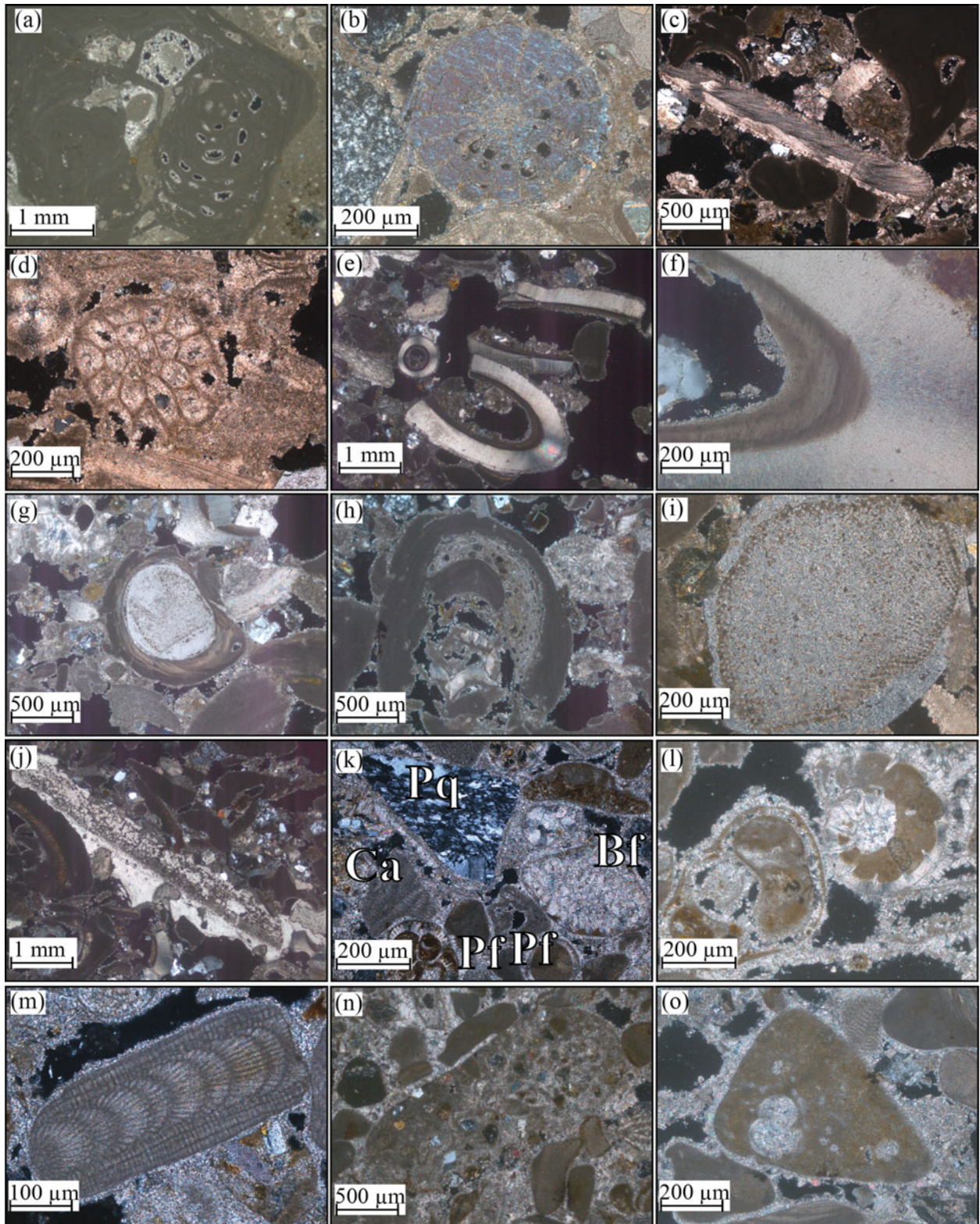


Figure 9. (Colour online) Photomicrographs of carbonate and clastic grains within the *Athalassa* (Gürpınar) Formation in the area studied: (a) calcareous red algae; (b) echinoderm plate; (c) bivalve fragment; (d) bryozoan; (e) reworked serpulid worm tubes; (f) algal growth on inner serpulid worm tube; (g) echinoderm with encrusting algae; (h) reworked clast of algae with encrusting calcareous red algae; (i) echinoderm plate with algal overgrowth; (j) echinoderm plate with algal overgrowth; (k) polycrystalline quartz [Pq], calcareous red algae [Ca], benthic foraminifera [Bf] and planktonic foraminifera [Pf]; (l) reworked benthic foraminifera with microbial cement infilling chambers; (m) reworked grain of calcareous red algae; (n) reworked grain of grainstone; and (o) reworked grain of marl with planktonic foraminifera.

algae (Fig. 9k–m), the latter occurring as well-rounded grains (Fig. 9m). Well-rounded, reworked clasts of grainstone, chalk and marl are also minor constituents of the grainstones (Fig. 9n, o).

The ratio of benthic to planktonic foraminifera in the B1 facies is typically *c.* 4:1 (based on point counting; R. N. Palamakumbura, unpub. Ph.D. thesis, Univ. Edinburgh, 2015). Most of the planktonic foraminifera show evidence of reworking (i.e. abrasion and fragmentation) from pre-existing deposits that were at least semi-lithified. The chambers within reworked foraminiferal tests are infilled with, and coated by, fine-grained (micritic) cement. In contrast, the cement of the grainstones as a whole is typically crystalline (sparitic) (Fig. 9k, l). Because of reworking, the total abundance of planktonic foraminifera cannot be used as a depth indicator. However, the presence of a few contemporaneous planktonic foraminifera is indicated by their well-preserved tests. The chambers within these foraminifera are infilled with sparite, similar to the cement of the lithology as a whole, suggesting contemporaneous diagenesis (and thus that these tests are not reworked).

8.a.2. Interpretation: very shallow-marine carbonate shelf

The B1 grainstone facies is interpreted as representing a fully marine deposit owing to the sedimentary structures present (e.g. well-preserved planar bedding) and the abundance of benthic foraminifera. The rarity of coeval planktonic foraminifera is consistent with deposition in shallow water (tens of metres at most) where a neritic fauna dominated. Horizons with abundant *Thalassinoides* are suggestive of periods of low net sediment accumulation. Channels were mostly infilled with medium-grained bioclastic sediment. In addition, lithified grainstone and marl blocks (*c.* 10–20 cm) were locally reworked along erosional surfaces. The evidence is indicative of localized mass-flow transport events from the Kyrenia Range into a shallow-marine shelf setting, along the northern margin of the basin.

The sedimentary features of the B2 facies rudstone (e.g. bioclastic grainstones) are interpreted to indicate accumulation on a gently sloping seafloor. The coralline red algal rhodoliths are likely to have formed, specifically in an inner to mid carbonate ramp environment, from which they were reworked down palaeoslope by high-energy events such as storms (cf. Pedley & Carrannante, 2006; Cornée *et al.* 2012). A similar depositional setting has been inferred, for example, for comparable Pliocene–Pleistocene deposits on Grande-Terre, an island in the French Lesser Antilles (Cornée *et al.* 2012).

The B3 packstone facies is interpreted to represent an inner to mid-carbonate ramp environment, owing to its mollusc-rich fauna and association with the B4 grainstone facies. The B4 grainstone facies is specifically interpreted to represent an inner carbonate ramp environment, owing to the well-preserved, low-angle cross-bedding and the occasional interbeds

of B3 packstone facies. Similar inner carbonate ramp facies have, for example, been described from SE Spain (Braga *et al.* 2006) and southern Italy (Nalin & Massari, 2009).

8.b. Deltaic facies

Deltaic facies make up a significant proportion of the higher levels of the Athalassa (Gürpınar) Formation (Fig. 5, logs 1 to 6) in the form of mass-flow-type deposits (facies C1) and fluvial deposits (facies C2).

The C1 facies comprises bioclastic conglomerates (Table 1) with variable proportions of bioclastic and siliciclastic material. The bioclastic debris includes bivalve shells such as *Ostrea*, *Cladocora* sp. (solitary coral), serpulid worm tubes, bryozoans and oncoids. In addition, reworked Miocene bivalves, including *Macrochlamys* sp. occur in the eastern Kyrenia Range (e.g. at Balalan (Platanissos) village; Fig. 2, log 1). Reworked Miocene corals such as *Tarbellastraea* are present in the western part of the Mesaoria (Mesarya) Plain (Fig. 2, log 6). The lithoclastic material ranges in size from 1 cm to 1 m, and is made up of sub-angular to sub-rounded clasts. A small proportion of the clasts within both the C1 and C2 conglomerate facies have been perforated by boring molluscs (Fig. 10a, b).

The C2 facies (Table 1) comprises conglomerate with well-rounded clasts, ranging in size from 1 to 10 cm (Fig. 10c). The conglomerate beds are thickest (>2 m) closest to the Kyrenia Range (*c.* 10 km) and generally become thinner (<10 cm) further from the range (>15 km) (Fig. 5, logs 2 to 7). These conglomerates are typically made up of normal-graded beds, 30 cm to 1 m-thick (Fig. 10c–e), with 30 to 50 cm-thick calcarenite interbeds. The conglomerates are clast-supported with a poorly lithified calcarenite matrix (*c.* 10% by volume). Poorly developed clast imbrication, as observed in the western part of the Mesaoria (Mesarya) Plain, suggests westward palaeoflow, away from the Kyrenia Range and towards the western coast (Fig. 5, log 4).

8.b.1. Conglomerate clast composition

The clast composition of the C1 and C2 conglomerate facies varies considerably, as observed near Balalan (Platanissos) village (Fig. 5, log 1), Kalkanlı (Kapouti) village (Fig. 5, logs 2 to 5), Güzelyurt (Morphou) town (Fig. 5, logs 5 and 6) and Gazimağusa (Famagusta) city (Fig. 5, logs 8 and 9). In decreasing order of abundance, the conglomerates near Balalan (Platanissos) village comprise basalt, serpentinite, radiolarite and chert, whereas those to the east of Kalkanlı (Kapouti) contain metacarbonate rock, sandstone, serpentinite, chert, basalt and grainstone. The conglomerates east of Güzelyurt (Morphou) contain diabase, jasper (iron-rich chert), sandstone, serpentinite, quartz, grainstone and chalk. The conglomerates near Gazimağusa (Famagusta) include clasts of metacarbonate rock, chalk, diabase, radiolarite and chert.

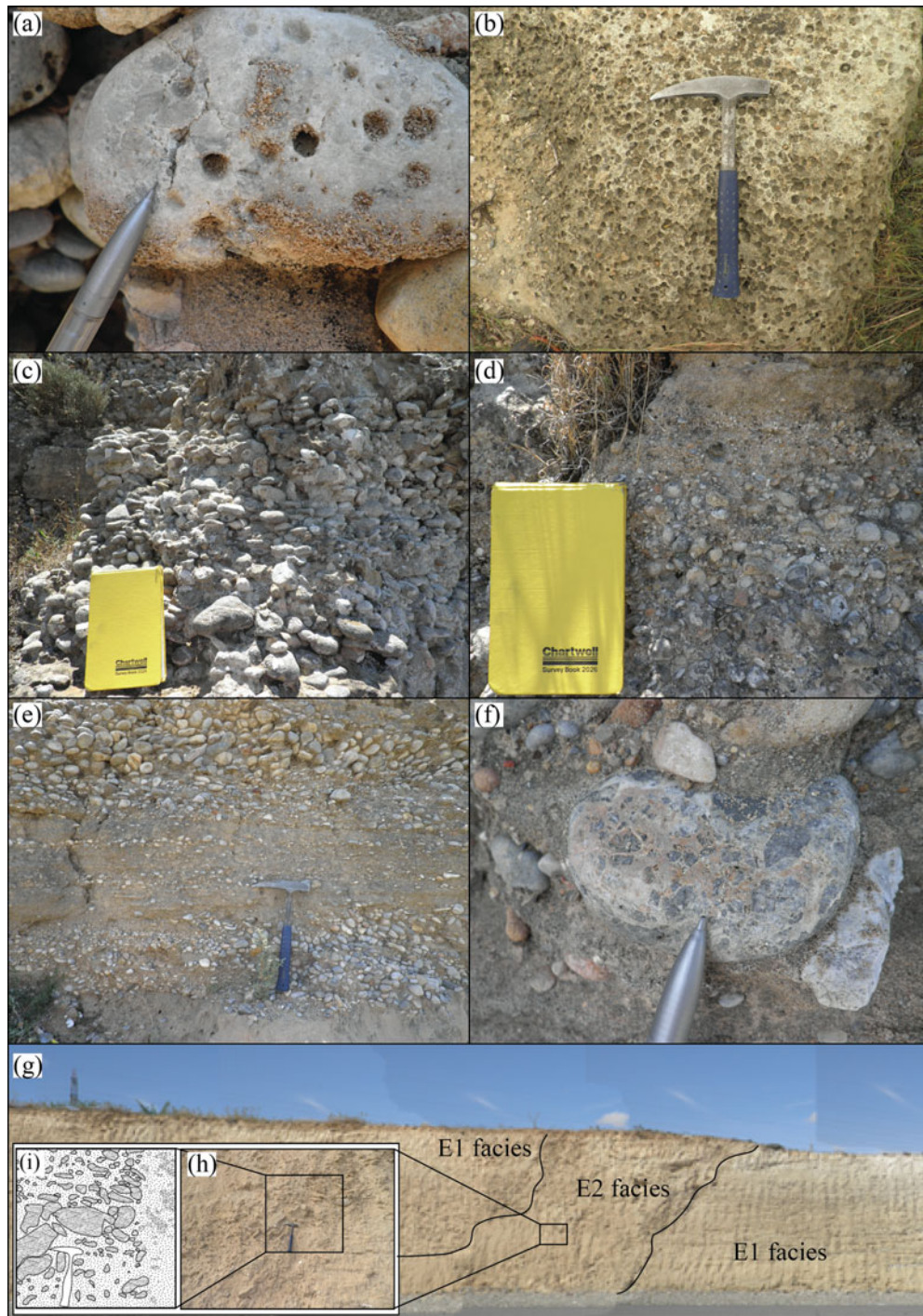


Figure 10. (Colour online) Photographs of key features of conglomerates within the Athalassa (Gürpınar) Formation in the area studied: (a) bored clast of metacarbonate; (b) heavily bored clast of grainstone; (c) well-rounded, clast-supported conglomerate (B2 facies); (d) normal grading within fluvial conglomerate beds (B2 facies); (e) interbedded conglomerate and calcarenite; (f) reworked clasts of megabreccia from the Pleistocene terraces (Palamakumbura & Robertson, 2016); (g) overview of a deposit comprising interbedded E1 and E2 facies; and (h, i) photograph and schematic sketch of the E2 facies breccia. Pencil length for scale is *c.* 15 cm, hammer head length is *c.* 30 cm and notebook length is *c.* 22 cm.

8.b.2. Interpretation: marine and non-marine deltas

The C1 bioclastic conglomerate facies is interpreted as a high-energy submarine mass-flow deposit. Taken together, the evidence suggests accumulation from short-lived, high-energy flows that reworked material, both from a continental setting and from a pre-existing marine setting. This interpretation is supported by the ab-

sence of sedimentary organization of the clasts, the angularity of most of the lithic material and the presence of a diverse marine macrofauna. Channels were scoured and then infilled by conglomerate. Some of the conglomerates are exposed near the Kyrenia Range, e.g. near Balalan (Platanissos) village (Figs 2, 5, log 1). This setting is consistent with the deposition of proximal submarine mass-flow deposits. Comparable

bioclastic conglomerates are reported from Miocene–Pliocene calcareous shelf deposits in coastal Israel (Buchbinder & Zilberman, 1997). The clasts there are poorly sorted and the bioclastic material includes coral, bivalves and gastropods.

The C2 conglomerate facies is interpreted as a shallow-marine, deltaic deposit, based on the presence of well-rounded clasts, planar bedding, normal grading of clasts and the occasional presence of contemporaneous neritic fossils. The palaeocurrent flow was generally towards the west. The clast lithologies indicate that the coarse material was mainly supplied from the metacarbonate rocks of the Trypa (Tripa) Group in the Kyrenia Range. The bored clasts were reworked from a pre-existing littoral marine environment. Similar fluvial drainage into a shallow-marine setting has been reported from Late Pleistocene temperate carbonate deposits, for example in southern Italy (Nalin & Massari, 2009), southern Greece (Kourampas & Robertson, 2000) and southern Cyprus (Poole & Robertson, 1998).

8.c. Lagoonal facies

Lagoonal facies are preserved directly north of the Ovgos (Dar Dere) fault zone in the northwest Mesaoria (Mesarya) Plain (Fig. 5, log 5). The deposits overlie the B1 to B4 facies grainstones and the C1 to C2 facies conglomerates. They comprise the D1 to D3 facies, which occur sequentially (Table 1). The D1 facies (Table 1) forms *c.* 3 m-thick sequences of thinly bedded grainstone, with 5 to 10 cm-thick parallel beds made up of carbonate and lithic grains (Fig. 5, log 5). The carbonate grains are mostly ostracods, molluscs, bryozoans and serpulid worm tubes. The D2 and D3 facies are both made up of floatstones comprising oysters and oncoids, respectively. The oyster floatstone (C2 facies) is dominated by *Ostrea*. The shells are commonly dissolved such that only casts remain (Fig. 6n). In contrast, the floatstone comprises well-preserved oncoids (Fig. 6o). The D2 and D3 facies form 30 cm to 1 m-thick depositional units that occasionally include lenses of B2 facies conglomerate (Fig. 5, log 5).

8.c.1 Interpretation: lagoonal to coastal setting

An overall low-energy, marine-influenced environment for the D1 grainstone facies is suggested by the regular centimetre-scale bedding. The mixed biota was derived from a range of open-marine to littoral settings. The mixing could reflect storm activity (Pedley & Grasso, 2002). In addition, the abundant lithic grains were derived from the metacarbonate rocks of the Trypa (Tripa) Group, as exposed in the central Kyrenia Range. The occasional lenticular conglomerates within the D1 facies grainstone are interpreted as channels (C2 facies), through which coarse clastic material was carried into small (hundreds of metres

long) shallow-marine lagoons by high-energy mass-flow processes.

The overlying D2 oyster floatstone facies is interpreted as a more restricted low-energy lagoonal environment. The abundance of *in situ* monospecific *Ostrea* shells is consistent with a low-salinity or fluctuating salinity environment. The inferred lagoons have counterparts, for example in Israel (Buchbinder & Zilberman, 1997) and west Sardinia (Andreucci *et al.* 2009).

The overlying D3 oncolitic facies is interpreted as representing inter-tidal to sub-tidal environments, owing to the abundance of oncoids to the exclusion of other biota (Wright, 1989; Alçiçek, Varol & Özkul, 2007). Similar Pleistocene lagoonal facies occur elsewhere, as in Iran (Djamali *et al.* 2006), near Granada in Spain (Martín-Algarra *et al.* 2003) and on the island of Mallorca, also in Spain (Ramos *et al.* 2001).

8.d. Carbonate aeolianites

Aeolian carbonate grainstone facies (E1 and E2) are developed in the upper part of the Athalassa (Gürpınar) Formation across the western and eastern parts of the Mesaoria (Mesarya) Plain and in the Karpaz (Karpas) Peninsula (Fig. 5). The E1 facies grainstone (Table 1) is fine to medium-grained and contains well-rounded carbonate and lithic grains. This facies is characterized by planar cross-bedding, with foresets dipping from 20° to 40° and ranging in thickness from 1 to 3 m (Table 1). The cross-bedding is locally separated by 1 to 2 m thick packages of grainstone, punctuated by 1 to 5 cm-spaced parallel bedding.

The E2 facies is only known in the western part of the Mesaoria (Mesarya) Plain, near the Ovgos (Dar Dere) fault zone (Fig. 5, log 6). The facies is composed of structureless, matrix-supported carbonate breccia (Table 1). The breccia forms tabular wedges, 1 to 8 m thick, interbedded with the E1 facies grainstone (Fig. 10g). The sedimentary breccia is dominated by angular clasts of grainstone, ranging in size from 1 to 50 cm, set in a matrix of medium-grained grainstone (Fig. 10h, i).

8.d.1. Interpretation of aeolian facies

The E1 grainstone facies is interpreted as representing coastal aeolian dunes owing to the well-rounded and well-sorted grains, the well-preserved, high-angle cross-bedding and the mixed bioclastic and lithic grain composition (as defined by Frébourg *et al.* 2008). The bioclastic grains are likely to have been sourced from locally exposed shallow-marine deposits, as represented by the B1 to B4 grainstone facies (see Section 8.a above). Comparable Pleistocene coastal carbonate aeolian deposits are known from numerous mid-latitude locations (Brooke, 2001), notably in tectonically uplifting areas, including Mallorca (Fornós *et al.* 2009), the Bahamas (Kindler & Mazzolini, 2001), Western Australia (Hearty & O'Leary, 2008) and southern Cyprus (Poole & Robertson, 2000).

The E2 grainstone breccia facies is interpreted as the result of localized downslope reworking of previously lithified E1 facies grainstone. This is inferred from the clast angularity, the absence of sedimentary organization, the restriction of clasts to a single lithology (E1 facies grainstone) and the presence of a locally steep palaeoslope between the E1 and E2 facies deposits (Fig. 10g). The presence of the E2 grainstone breccia facies represents a period of reworking prior to further aeolian deposition.

9. Sedimentary evolution of the northern Mesaoria (Mesarya) Basin

Each outcrop area exposes different depositional environments within the northern part of the Mesaoria (Mesarya) Basin, namely: (1) shallow, proximal parts of the basin near the Kyrenia Range, (2) deeper, more distal parts of the basin in the east, and (3) a carbonate ramp system that developed directly south of the Ovgos (Dar Dere) fault zone.

9.a. Karpaz (Karpas) Peninsula: a proximal part of the basin

Two sedimentary environments are preserved on the Karpaz (Karpas) Peninsula in the far east of the basin: firstly, deposits that overlie the eastern extension of the range, and secondly deposits along the southern coast of the peninsula. The deposits overlying the range are characterized by the B4 facies cross-bedded grainstone, which is interpreted as representing a very shallow-marine environment. Locally interbedded bioclastic conglomerate, containing both bioclastic and lithic material, resulted from channelized mass-flows into a shallow-marine environment. Reworked Miocene bivalves (*Macrochlamys* sp.) are indicative of a pre-existing shallow-marine setting in this area, which is today not exposed in the Karpas Peninsula. In addition, the well-exposed B1 facies grainstone along the southern coast of the Karpaz (Karpas) Peninsula is interpreted as representing an open-marine environment.

9.b. Eastern part of the Mesaoria (Mesarya) Basin: deeper part of the basin

The eastern part of Mesaoria (Mesarya) Basin is interpreted as an open, shallow-marine shelf, taking account of the interbedded benthic foraminifera-rich grainstone and marl sequences. Localized, highly bioturbated horizons and variable concentrations of *in situ* molluscs suggest a variable sedimentation rate, possibly reflecting relative changes in sea level. The reworked clasts of grainstone and marl within lenticular bodies are suggestive of periodical high-energy events (e.g. storms) which involved the localized cutting and filling of subaqueous channels. The lithic material in the channelized conglomerate was derived from the Kyrenia Range, which was by then emerging.

The overlying open-marine, cross-bedded grainstones (B4 facies) and packstone (B3 facies) were succeeded by coastal aeolian dunes. The overall sequence in the northeast of the basin, therefore, records shallowing upwards from open marine to shallow marine, and finally to an aeolian setting.

9.c. Carbonate ramp in the northwest of the basin

In the northwestern Mesaoria (Mesarya) Basin, the B1 to B4 facies are interpreted as a *c.* NE–SW-trending shallow-marine, cool-water carbonate ramp that developed directly south of the E–W-trending Ovgos (Dar Dere) fault zone (Fig. 11).

Strike-slip movement is inferred to have characterized the Ovgos (Dar Dere) fault zone during Late Miocene time (Harrison *et al.* 2004; McCay & Robertson, 2013). The sedimentary evidence suggests that an E–W-trending topographic high developed parallel to the fault zone (McCay & Robertson, 2013). This, in turn, implies some degree of contemporaneous transpression along the Ovgos (Dar Dere) fault zone to cause local uplift in this area. The topographic high was bordered by a southward palaeoslope on which the carbonate ramp developed. The northern limit of this ramp was delimited by a fault-controlled ridge of chalk (Fig. 7). The carbonate ramp deepened southwards away from the fault zone. Exposure is inadequate to determine if the carbonate ramp extended laterally across the Mesaoria (Mesarya) Basin parallel to the Ovgos (Dar Dere) fault zone. The scale of the carbonate ramp (<1 km across) is similar to other Pliocene and Pleistocene examples in the Mediterranean region (Pedley & Grasso, 2002; Braga *et al.* 2006; Nalin & Massari, 2009).

Four main stages of carbonate ramp development can be inferred from the exposed facies:

Stage 1: Calcareous red algal rudstone and benthic foraminifera-rich grainstone accumulated to form the upper, mid and lower parts of the carbonate ramp (Fig. 11a), in line with the depositional model of Pedley & Carannante (2006). Mollusc- and coral-rich deposits represent the shallowest, most proximal parts of the ramp environment, whereas benthic foraminifera-rich grainstone, as observed in the south, represent more distal parts of the carbonate ramp. Unfortunately, no strandline deposits are preserved in the outcrops studied, probably because of erosion of the topographic high along the fault zone.

Stage 2: Erosional surfaces, bored clasts and extensive burrowing along a specific horizon within the inferred lower ramp facies (Fig. 11b) and are interpreted to represent periods of relatively low sediment accumulation. The Kyrenia Range hinterland was subaerially exposed by this time, as indicated by the reworking of bioclastic and lithic material into a shallow-marine environment by high-energy mass-flow processes (Fig. 11b). Comparable lower ramp facies have been described from southern Italy and interpreted similarly (Nalin & Massari, 2009).

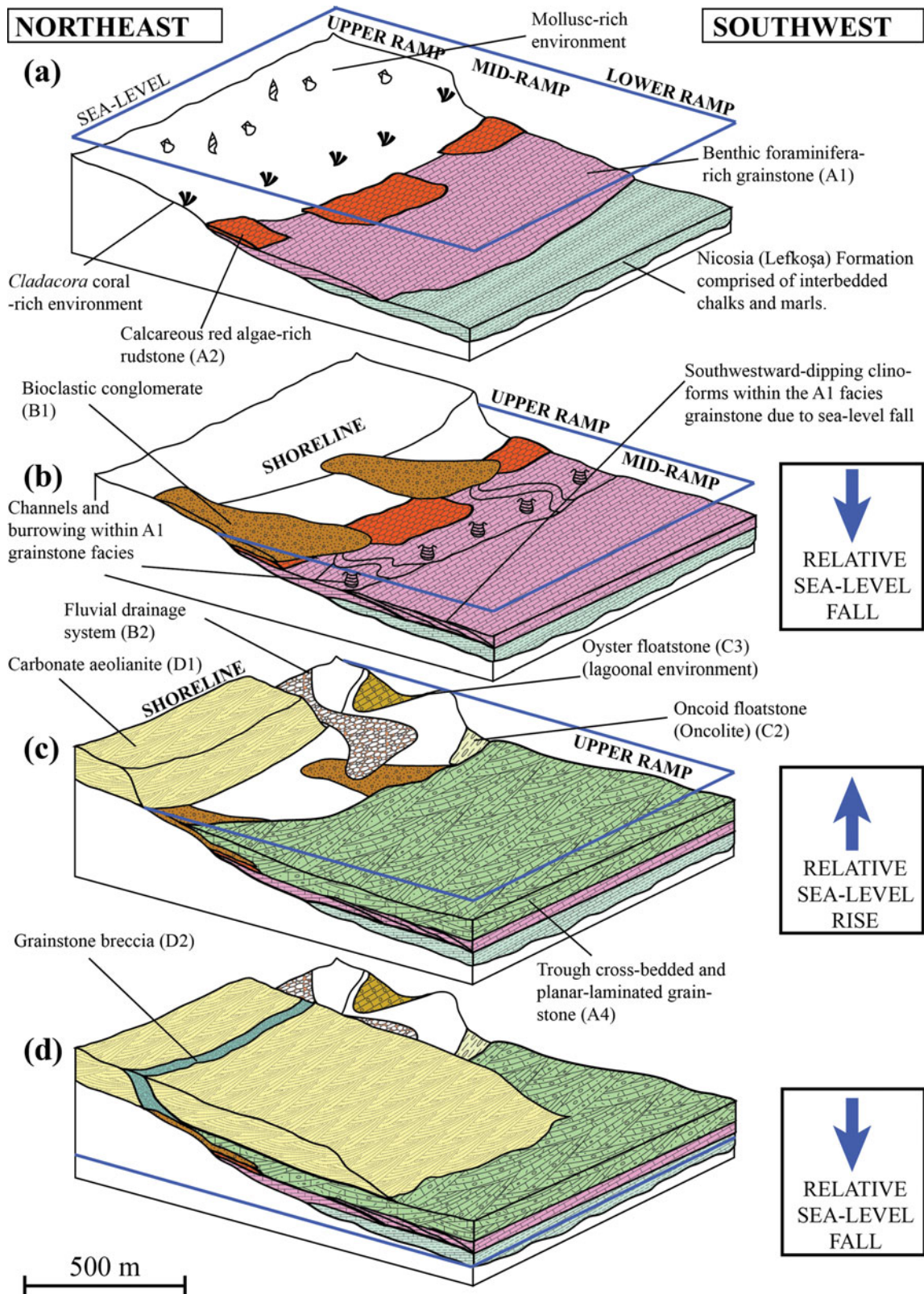


Figure 11. (Colour online) Depositional model of the Pleistocene development of a cool-water carbonate ramp in the northwest part of the Mesaoria (Mesarya) Basin.

Shallowing-upward clinoforms with seaward-dipping upper surfaces are well preserved within the B1 facies grainstone. These shallowing-upward features are likely to reflect glacio-eustatic sea-level change (although the effects of autocyclic ramp con-

struction or tectonic movements cannot be excluded). In addition, the bioclastic conglomerates in the upper part of the sequence are inferred to record subaerial exposure (Fig. 11b). The implied relative sea-level fall is likely to represent an example of a forced

regression. Forced regressions within shallow-marine sequences are known to result in progressive shallowing of clinoforms, seaward-dipping upper bounding surfaces and long-distance regression (Posamentier & Morris, 2000). Similar, depositional features in other sequences are also interpreted as forced regressions, including examples in Sicily (Massari & Chiocci, 2006), the northeast Gulf of Mexico (Kolla *et al.* 2000), SE Italy (Tropeano & Sabato, 2000) and Rhodes (Hansen, 1999).

Stage 3: The mid to inner carbonate ramp deposits were unconformably overlain by trough cross-bedded grainstone (B4 facies), oyster floatstone (D2 facies) and oncolitic facies (D3 facies). This is suggestive of a relative sea-level rise, which resulted in re-submergence of the carbonate ramp (Fig. 11c). The trough cross-bedding indicates generally east to west palaeoflow (Fig. 5, log 4), which is likely to reflect deepening towards the open Mediterranean Sea. The fluvial deposits that are interbedded with the B4 facies grainstone are indicative of sediment supply from the Kyrenia Range into a shallow-marine, deltaic environment (Fig. 11c). The oyster floatstone and oncolite facies, which are only preserved above the most northerly part of the carbonate ramp sequence, record lagoonal deposition during a regression that culminated in emergence.

Stage 4: Aeolian grainstones accumulated after final marine regression (Fig. 11d). Carbonate aeolian dunes formed near the northeastern margin of the ramp sequence (Fig. 11d). In the lower (southeasterly) parts of the ramp, aeolian grainstone first appears above a prominent erosion surface. This was covered, first by erosional talus (E2 facies grainstone breccia) and then by typical aeolian grainstones. A locally steep palaeosurface (5 m high and *c.* 30–45°) is likely to represent coastal erosion during or soon after final emergence. The carbonate ramp (and its likely non-exposed lateral extension) is interpreted as the main source of bioclastic carbonate material within the non-marine deposits.

Also of note is the presence of reworked *Tarbellastraea* (coral) within the western part of the Mesaoria (Mesarya) Basin. This shows that neritic carbonates accumulated during Miocene time in this area, although no such deposits are now preserved to the north of the Troodos Massif. Combined with the evidence of Miocene molluscs in the west (see above), this indicates that shallow-marine deposits accumulated widely along the present southern margin of the Kyrenia Range but were eroded during later uplift.

10. Comparison with the southern part of the basin

Pliocene–Pleistocene exposures in the southern part of the Mesaoria (Mesarya) Plain, which borders the northern periphery of the Troodos Massif, have previously been described and interpreted in some detail (Ducloz, 1965; McCallum & Robertson, 1990, 1995a,b; Schirmer *et al.* 2010; Weber *et al.* 2011;

Kinnaird, Robertson & Morris, 2011). Where locally exposed along the periphery of the Troodos Massif, Messinian gypsum is overlain, first by hemipelagic marls that record initial marine transgression after the Messinian salinity crisis (Follows & Robertson, 1990) and then by open-marine shelf-depth calcareous mudrocks of the Nicosia (Lefkoşa) Formation (McCallum & Robertson, 1990). Biostratigraphic studies using planktonic foraminifera and calcareous nanoplankton indicate a Pliocene age, encompassing nanofossil zones 17 and 18 (Lord, Panayides & Xenophontos, 2000). The marls and mudrocks are locally intercalated with lenticular conglomerates, which are dominated by rounded pebble- to cobble-sized clasts of Troodos-derived igneous rocks, especially diabase. These rudaceous sediments are interpreted as small, subaqueous channels within prograding fan deltas (McCallum & Robertson, 1990). In addition, relatively small lenses of bioclastic carbonate in some basin-margin areas are inferred to have been swept in from littoral deposits to the south by high-energy processes (i.e. storms). The sediment packaging is likely to have been influenced by glacio-eustatic sea-level change, although an improved age resolution is needed to test this hypothesis.

Conformably overlying the Nicosia (Lefkoşa) Formation along the northern periphery of the Troodos Massif is the Kakkaristra Formation (10–15 m thick) (Ducloz, 1965; McCallum & Robertson, 1995b). This is dominated by channelized conglomerates that are interbedded with finer-grained deposits, which in places include marine bivalves (e.g. *Ostrea*), ostracods and plant debris. The Kakkaristra Formation is interpreted as a northward-prograding shallow-marine fan-delta sequence (McCallum & Robertson, 1995b). In the south (i.e. south of Nicosia), the Kakkaristra Formation is overlain by the Apalos Formation (*c.* 45.5 m thick) (Ducloz, 1965; McCallum & Robertson, 1990; Schirmer *et al.* 2010), which is dominated by channelized, non-marine conglomerates that are interbedded with inferred overbank deposits, palaeosols, and minor lacustrine and aeolian deposits. The Apalos Formation is interpreted as a non-marine fan-delta sequence, which prograded northwards into the Mesaoria (Mesarya) Basin (McCallum & Robertson, 1995b).

Further north (e.g. in the Greater Nicosia (Lefkoşa) area) the Pliocene Nicosia (Lefkoşa) Formation is seen in outcrop to pass depositionally upwards into the Athalassa (Gürpınar) Formation (*c.* 80 m thick) (McCallum & Robertson, 1995a). The formation comprises a lower member that accumulated in a shallow-marine environment and an upper member that is interpreted as a series of southward-migrating bioclastic carbonate sand waves within a shallow sea. The upper part of the Athalassa (Gürpınar) Formation, as exposed in the Greater Nicosia (Lefkoşa) area, includes oyster-rich deposits and thin conglomerate beds with pebble-sized clasts set in a bioclastic matrix (McCallum & Robertson, 1995a). These deposits are interpreted to have accumulated in a lagoonal environment, together

with reworked shoreface or near-shoreface conglomeratic deposits. Overall, the Athalassa (Gürpınar) Formation accumulated within a dwindling shallow-marine seaway between the Kyrenia Range and the Troodos Massif. The succession culminated in emergence and a switch to deposition of coarse non-marine clastic material, which was derived from the Troodos Massif.

11. Palaeogeography of the Mesaoria (Mesarya) Basin

The overall distribution of the Pliocene–Pleistocene facies of the Mesaoria (Mesarya) Basin is summarized in Figure 12a, and the inferred palaeoenvironments in Figure 12b. In addition, an inferred cross-section of the Lower Pleistocene deposits, from the Troodos Massif to the Kyrenia Range, is shown in Figure 13b. Deposits are lacking in some areas, including the central part of the northern margin of the basin and the northern flank of the Kyrenia Range, requiring inferences of the likely palaeogeography.

The chalks and marls of the Nicosia (Lefkoşa) Formation underlie the Athalassa (Gürpınar) Formation in both the northern and southern parts of the basin. Near the southern margin of the basin the Nicosia (Lefkoşa) Formation is up to 900 m thick, whereas, in strong contrast, the exposed deposits in the northern part of the basin, described above, are no more than 16 m thick (Fig. 13b). Borehole data from south of the Ovgos (Dar Dere) fault zone confirm that the Nicosia (Lefkoşa) Formation is thickest to the south of the fault zone but is vastly thinner between the fault zone and the Kyrenia Range (McCallum & Robertson, 1995a; Harrison *et al.* 2008; see Fig. 13b). The basin was, therefore, compartmentalized, with much thicker deposits to the south of the Ovgos (Dare Dere) fault zone compared to the north of the fault zone.

Channels within the Nicosia (Lefkoşa) Formation near the southern margin of the Mesaoria (Mesarya) Basin contain material derived from the Troodos Massif. The composition and the well-rounded nature of the clasts suggest that they were derived from an emergent landmass to the south of the basin. In contrast, conglomerate channels are not preserved within the contemporaneous chalks and marls of the Nicosia (Lefkoşa) Formation in the northern part of the basin. This suggests that the Kyrenia Range did not significantly emerge above sea level until Pleistocene time.

Overlying the Nicosia (Lefkoşa) Formation in both the northern and southern parts of the basin are the various facies of the Athalassa (Gürpınar) Formation (Figs 12, 13b). In the south, the coastline was located near the northern margins of the Kakkariastra marine fan deltas at an early stage and, later near the edge of the non-marine Apalos fan deltas. In the north, the coastline approximately followed the Ovgos (Dar Dere) fault zone, as suggested by the preserved near-coastal deposits (Fig. 12a, b). The basin floor dipped southwards away from the fault zone allowing the carbonate ramp to develop along the northwestern margin

of the basin, although it may also have existed more widely (Figs 12, 13b).

The area between the Kakkariastra fan deltas in the south and the Ovgos (Dar Dere) fault zone in the north encompassed an E–W-trending seaway in which the shallow-marine facies of the Athalassa (Gürpınar) Formation accumulated (McCallum & Robertson, 1995a). Within these shallow-marine deposits as a whole, lithoclastic material was locally derived from the Kyrenia Range (e.g. metacarbonate rock of the Trypa (Tripa) Group), suggesting that this lineament had emerged above sea level by Early Pleistocene time (Fig. 13b). The thick cross-bedded grainstones are especially well preserved in the southern part of the basin, an area that experienced southward-directed palaeoflow (Figs 12, 13b). Somewhat deeper, open-marine deposits accumulated in the eastern and western parts of the basin (Fig. 12). With time, the sea regressed leaving only oyster-rich deposits in semi-enclosed lagoons, as exposed in the Greater Nicosia area (Figs 12b, 13b) (McCallum & Robertson, 1995a).

The Karpaz (Karpas) Peninsula represents the northern margin of the offshore, eastward extension of the Mesaoria (Mesarya) Basin. Deposits within this area encompass lagoonal facies, high-energy debris-flow deposits and shallow-marine deposits (Fig. 12a). The depositional setting deepened slightly from very shallow-marine to open-marine (but still shallow) further south (Fig. 12b).

In the northwest, shallow-marine deposits, notably trough cross-bedded grainstones, are preserved in the topographically subdued westward extension of the Kyrenia Range, represented by the Koruçam Burnu (Cape Kormakiti) area (Fig. 12). Similar deposits crop out northwards for several kilometres to the north coast of the island (Fig. 12a), indicating that the westernmost part of the Kyrenia Range remained submerged during Early Pleistocene time. Similar shallow-marine deposits may have extended along the northern flank of the Kyrenia Range but, if so, are not preserved (Fig. 12b). Later during Early Pleistocene time, the Kyrenia Range lineament underwent surface uplift resulting in the southward progradation of deltas, marine regression, the formation of small lagoons, and finally a switch to aeolian deposition (Fig. 12b). Recent sedimentary and palaeomagnetic evidence from the periphery of the Troodos Massif (McCallum & Robertson, 1995b; Schirmer *et al.* 2010; Kinnaird, Robertson & Morris, 2011; Weber *et al.* 2011), combined with new evidence from the Kyrenia Range (Palamakumbura & Robertson, 2016; Palamakumbura *et al.* 2016b), indicate that the two areas uplifted contemporaneously from Early Pleistocene time onwards.

12. Previous tectonic–sedimentary models of the Mesaoria (Mesarya) Basin

Previous tectonic models of the Mesaoria (Mesarya) Basin, especially those proposed by McCallum &

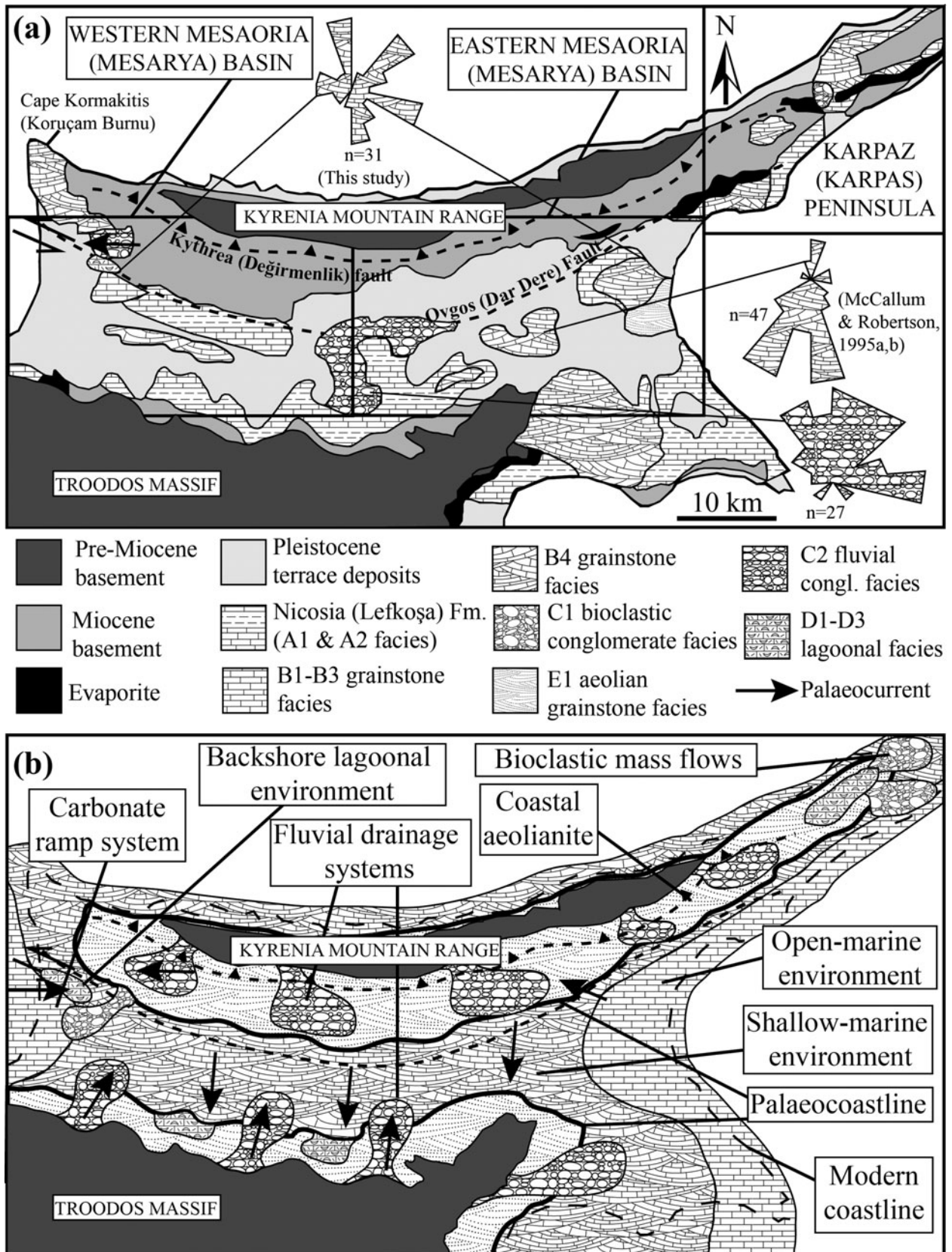


Figure 12. Summary maps showing: (a) the distribution of the various facies of the Athalassa (Gürpınar) Formation, and (b) an interpretation of the palaeogeography of the Mesaoria (Mesarya) Basin during Early Pleistocene time.

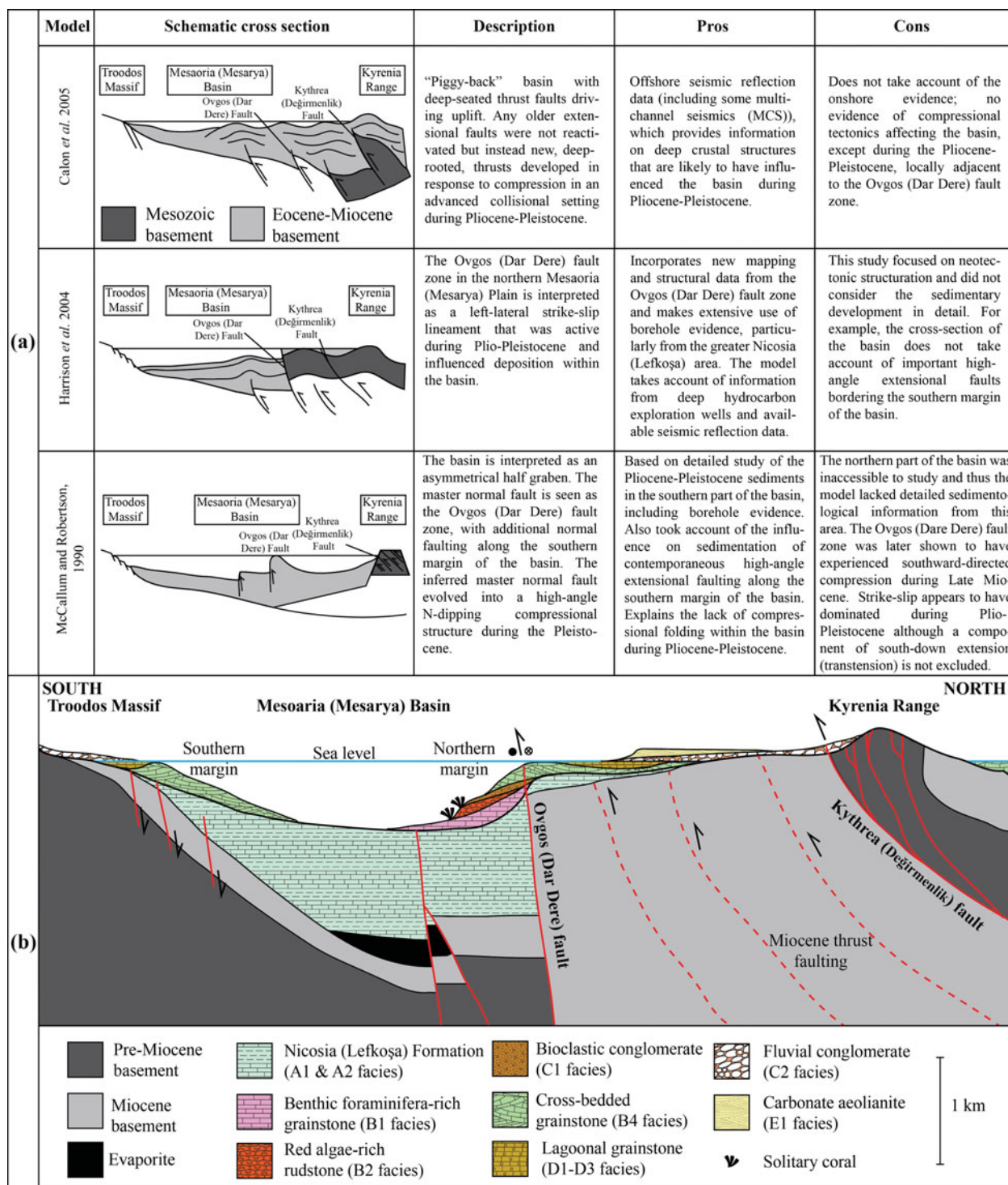


Figure 13. (Colour online) (a) Overview of the various models for the Plio-Pleistocene structure of the Mesaoria (Mesarya) Basin, with a summary evaluation of each model. (b) Schematic section through the Mesaoria (Mesarya) Basin during Early Pleistocene time, illustrating various facies relationships near the northern and the southern margins of the basin. The pre-Pliocene structure of the basin is adapted from Harrison *et al.* (2004) and Robertson & Kinnaird (2016).

Robertson (1990), by Calon, Aksu & Hall (2005) and by Harrison *et al.* (2004) are summarized and briefly evaluated in Figure 13a. No one of these models satisfactorily explains all aspects of the basin development. In particular, the half-graben model of McCallum & Robertson (1990) did not take account of evidence from the, then inaccessible, Ovgos (Dare Dere) fault zone, which has since been interpreted as a sinis-

tral strike-slip lineament (Harrison *et al.* 2004). There is no evidence of regional-scale folding and thrusting within the Pliocene–Pleistocene deposits of the Mesaoria (Mesarya) Basin, which is at odds with the advanced continental collisional model of Calon, Aksu & Hall (2005). In addition, the strike-slip-controlled basin model (Harrison *et al.* 2004) does not take account of the evidence of *c.* E–W and *c.* N–S high-angle

normal faulting along the southern margin of the Mesaoria (Mesarya) Basin, and of comparable normal faulting in the south of Cyprus (Follows & Robertson, 1990; Kinnaird & Robertson, 2013).

13. Tectonic–sedimentary development of the Mesaoria (Mesarya) Basin

Combined with published information, our new sedimentological evidence and interpretation provide the basis for a new interpretation of the Mesaoria (Mesarya) Basin development. Any interpretation must take account of sub-surface data from water wells and exploratory hydrocarbon wells (McCallum & Robertson, 1990; Harrison *et al.* 2004).

The Mesaoria (Mesarya) Basin, as shown in Figure 13b, was initiated during Late Miocene – earliest Pliocene times as a flexurally controlled fore-deep related to southward thrusting and folding of the Kyrenia Range in a left-lateral transpressional setting (McCay & Robertson, 2013). The effective southern limit of the zone of major compressional deformation was the Ovgos (Dar Dere) fault zone, which locally shows evidence of southward-directed compression (Harrison *et al.* 2004; McCay & Robertson, 2013). During Messinian time, the Mesaoria (Mesarya) Basin existed as a pronounced depocentre to the south of the Ovgos (Dar Dere) fault zone, in which evaporites, including halite, accumulated to a thickness of *c.* 70 m (Pantazis, 1978; Robertson *et al.* 1995; Necdet & Anil, 2006). Evidence from the evaporites indicates that compressional deformation was active during Messinian time within and adjacent to the Kyrenia Range. The deformation appears to have continued into earliest Pliocene time, based on facies evidence from near the Kyrenia Range front (McCay & Robertson, 2013).

The northern margin of the Troodos Massif experienced down-to-the-N high-angle faulting (ENE–WSW-striking normal faults) during Late Miocene – Early Pliocene time, cumulatively reaching hundreds of metres of displacement (Follows & Robertson, 1990; Kinnaird & Robertson, 2013). Extensional faulting of the Troodos Massif continued into Early Pliocene time as indicated by faulting in marls in the lower part of the Nicosia (Lefkoşa) Formation (Follows & Robertson, 1990; Kinnaird & Robertson, 2013). It is likely that tectonically controlled subsidence within the unexposed central segment of the Mesaoria (Mesarya) Basin, to the south of the Ovgos (Dar Dere) fault zone, also continued during Early–Late(?) Pliocene time, producing much of the accommodation space needed for nearly 900 m of chalks and marls of the Nicosia (Lefkoşa) Formation. During later Pliocene to Early Pleistocene times, the Mesaoria (Mesarya) Basin appears to have been passively infilled, accompanied by compaction and lithostatic subsidence. This is consistent with the absence of contemporaneous faulting within the exposed basin fill, other than along the Ovgos Fault (Dar Dere) strike-slip lineament.

As a result of its Late Miocene to Pliocene development, the Mesaoria (Mesarya) Basin infill is thick (*c.* 900 m) within the subsided area in the south of the overthrust load, but very much thinner (<16 m) overlying the former thrust load to the north of the Ovgos (Dar Dere) fault zone. By Early Pleistocene time, after its infill as a whole, the Mesaoria (Mesarya) Basin developed into a shallow-marine shelf. This was followed by marine regression and intense uplift of both the Kyrenia Range and the Troodos Massif.

A related outcome of this study is that we suggest that the stratigraphy of the Pliocene and Pleistocene deposits, as originally devised by Ducloz (1965), with later modifications (Baroz, 1979; McCallum & Robertson, 1990) should be retained in preference to an alternative stratigraphy proposed by Harrison *et al.* (2004). The main reason is that the Nicosia (Lefkoşa) Formation is everywhere overlain by the traditional Athalassa (Gürpınar) Formation, which forms a mappable unit wherever exposed in Cyprus. We did not observe any intercalations of bioclastic carbonate rocks within the Nicosia (Lefkoşa) Formation in the northern part of the Mesaoria (Mesarya) Basin, which would support a reassignment of the Athalassa (Gürpınar) Formation as a member of an extended Nicosia (Lefkoşa) Formation, as proposed by Harrison *et al.* (2004).

14. Regional tectonic development of the Mesaoria (Mesarya) Basin

The basin was initiated by southward collision-related thrusting of the Kyrenia lineament to form a flexurally controlled foredeep (Fig. 14a). However, the cumulative throw on the *c.* E–W normal faults within the foreland, represented by the northern margin of the Troodos Massif, greatly exceeds that expected for a typical foreland basin (Stockmal & Beaumont, 1987). The probable explanation is that the Troodos Massif did not simply represent a marginal backstop, but instead also experienced extension related to subduction to the south, as seen in the high-angle faults along the southern margin of the Troodos Massif (Kinnaird & Robertson, 2013).

Ongoing diachronous convergence of the African and Eurasian plates resulted in the well-documented westward tectonic escape of Anatolia along the Northern and Eastern Anatolian Fault Zones (NAFZ and EAFZ) during Pliocene and Pleistocene times (Figs 1, 14b) (Şengör, Görür & Saroğlu, 1985). By Late Miocene time the Ovgos (Dar Dere) fault zone was active as a strike-slip fault zone, in effect delineating the northern boundary of the Mesaoria (Mesarya) Basin (Fig. 14b). The Early to Late(?) Pliocene infill of the basin is likely to have taken place in a sinistral transtensional setting.

The Eratosthenes Seamount is inferred to have collided with the Cyprus Trench to the south of the island during Late Pliocene – Pleistocene times (Robertson,

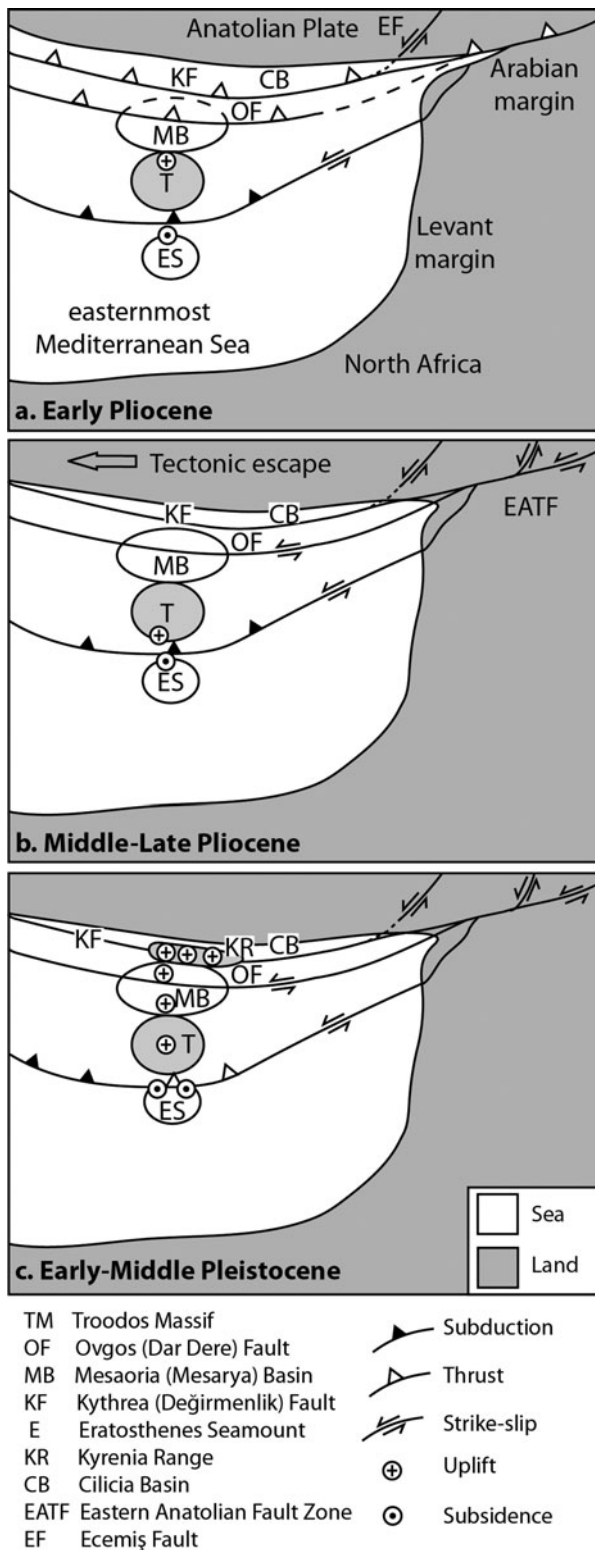


Figure 14. Plate tectonic sketch map showing the inferred regional tectonic setting of the Mesaoria (Mesarya) Basin in the Eastern Mediterranean during Pliocene and Pleistocene times.

1998). This collision is seen as the main driving force of rapid uplift and final emergence of the Troodos Massif to the south of the Mesaoria (Mesarya) Basin (Fig. 14c).

15. Conclusions

New facies evidence from the northern margin of the Mesaoria (Mesarya) Basin, when combined with existing data from the southern part of the basin, allows the first comprehensive synthesis of the basin evolution in its regional tectonic setting during Pliocene–Pleistocene times.

(1) The Mesaoria (Mesarya) Basin (as defined here) represents the Pliocene to Pleistocene infill of a basin between two tectonically active lineaments to the north and south, represented by the Troodos Massif and the Kyrenia Range.

(2) The Mesaoria (Mesarya) Basin was activated during Late Miocene time as a flexural basin in an early-stage collisional setting.

(3) Within the depocentre, the deposits reach *c.* 900 m in thickness, based on borehole evidence, whereas they are much thinner (*c.* 16 m) in the northern part of the basin, to the north of the regionally important *c.* E–W-trending Ovgos (Dar Dere) fault lineament.

(4) The presence of Lower to Late-Pliocene chalks and marls making up the Nicosia (Lefkoşa) Formation in the northern part of the basin indicates that the Kyrenia Range remained submerged during Pliocene time. In contrast, the Troodos Massif was by then emergent to the south of the basin.

(5) The change from chalks and marls of the Nicosia Formation to shallow-marine, mostly bioclastic deposits of the Athalassa (Gürpınar) Formation represents an abrupt shallowing of the basin around the Pliocene–Pleistocene boundary, which is attributed to regional tectonic uplift.

(6) Further shallowing from open-marine to semi-enclosed marine and finally to non-marine settings is indicative of further Pleistocene uplift.

(7) Strike-slip/transpression along the Ovgos (Dar Dere) fault zone near the northern margin of the basin influenced the development of a SW-dipping cool-water carbonate ramp in which stages of initial development, forced regression, re-submergence and final emergence are recognized based on facies evidence.

(8) The Mesaoria (Mesarya) Basin records the infill of a flexurally controlled foredeep that formed during Late Miocene –earliest Pliocene early-stage collision. The Early–Late(?) Pliocene basin infill is likely to have taken place in a transtensional setting, influenced by sinistral strike-slip along the Ovgos (Dar Dere) fault lineament in the north during Pliocene time, controlled by the westward tectonic ‘escape’ of Anatolia towards the Aegean region. The subsequent Pleistocene uplift of the basin relates to the collision of the leading edge of the North African continent, represented by the Eratosthenes Seamount, with the Cyprus Trench to the south.

(9) Syn-collisional basins may, therefore, show strong changes in prevailing structural control within short time periods, which may be relevant to the

interpretation of other collisional settings, for example in the Tethyan region elsewhere or Iapetus.

Acknowledgements. The first author was in receipt of a NERC CASE award held at the University of Edinburgh. The work was assisted by a financial contribution from the John Dixon Memorial Fund. Both authors acknowledge scientific discussions with, amongst others Prof. Dick Kroon, Prof. Rachel Wood and Dr Martyn Pedley. We thank Prof. Kemal Tasli and Prof. Nurdan İnan (Mersin University, Turkey) for helping with the identification of planktonic and benthic foraminifera. Finally, we thank Dr Mehmet Necdet (Geology and Mines Dept., Lefkoşa (Nicosia)) for assistance during our fieldwork in Cyprus.

References

- ALÇIÇEK, H., VAROL, B. & ÖZKUL, M. 2007. Sedimentary facies, depositional environments and palaeogeographic evolution of the Neogene Denizli Basin, SW Anatolia, Turkey. *Sedimentary Geology* **202**, 596–637.
- ANDREUCCI, S., PASCUCCI, V., MURRAY, A. S. & CLEMMENSEN, L. B. 2009. Late Pleistocene coastal evolution of San Giovanni di Sinis, west Sardinia (Western Mediterranean). *Sedimentary Geology* **216**, 104–16.
- BAROZ, F. 1979. *Etude géologique dans le Pentadaktylos et la Mesaoria (Chypre Septentrionale)*. Université de Nancy. Published thesis.
- BEAUMONT, C. 1981. Foreland Basins. *Geophysical Journal International* **65**, 291–329.
- BRAGA, J. C., MARTIN, J. M., BETZLER, C. & AGUIRRE, J. 2006. Models of temperate carbonate deposition in Neogene basins in SE Spain: a synthesis. In *Cool-water Carbonates: Depositional Systems and Palaeoenvironmental Controls* (eds H. M. Pedley & G. Carannante), pp. 121–35. Geological Society of London, Special Publication no. 255.
- BROOKE, B. 2001. The distribution of carbonate eolianite. *Earth-Science Reviews* **55**, 135–64.
- BUCHBINDER, B. & ZILBERMAN, E. 1997. Sequence stratigraphy of Miocene–Pliocene carbonate-siliciclastic shelf deposits in the eastern Mediterranean margin (Israel): effects of eustasy and tectonics. *Sedimentary Geology* **112**, 7–32.
- CALON, T. J., AKSU, A. E. & HALL, J. 2005. The Oligocene–Recent evolution of the Mesaoria Basin (Cyprus) and its western marine extension, Eastern Mediterranean. *Marine Geology* **221**, 95–120.
- COHEN, K. M. & GIBBARD, P. L. 2010. *Global Chronostratigraphical Correlation Table for the Last 2.7 Million Years*. Cambridge, England: Subcommission on Quaternary Stratigraphy (International Commission on Stratigraphy).
- CONSTANTINO, G. 1995. *Geological Map of Cyprus*. Nicosia: Geological Survey of Cyprus.
- CORNÉE, J. J., LÉTICÉE, J. L., MÜNCH, P., QUILLÉVÉRÉ, F., LEBRUN, J. F., MOISSETTE, P., BRAGA, J. C., MELINTE-DOBRIŃESCU, M., DE MIN, L., OUDET, J. & RANDRIANASOLO, A. 2012. Sedimentology, palaeoenvironments and biostratigraphy of the Pliocene–Pleistocene carbonate platform of Grande-Terre (Guadeloupe, Lesser Antilles forearc). *Sedimentology* **59**, 1426–51.
- DJAMALI, M., SOULIÉ-MÄRSCH, I., ESU, D., GLIOZZI, E. & OKHRAVI, R. 2006. Palaeoenvironment of a Late Quaternary lacustrine–palustrine carbonate complex: Zarrand Basin, Saveh, central Iran. *Palaeogeography, Palaeoclimatology, Palaeoecology* **237**, 315–34.
- DUCLOZ, C. 1965. *Revision of the Pliocene and Quaternary Stratigraphy of the central Mesaoria*. Nicosia. Cyprus Geological Survey Department Report for 1964, pp. 31–42.
- DUCLOZ, C. 1972. The Geology of the Bellapais-Kythrea area of the Central Kyrenia Range. *Bulletin of the Cyprus Geological Survey Department* **6**, 44–71.
- FOLLOWS, E. & ROBERTSON, A. 1990. Sedimentology and structural setting of Miocene reefal limestones in Cyprus. In *Ophiolites: Oceanic Crustal Analogues, Proceedings of the Symposium “Troodos 1987”* (eds J. Malpas, E. M. Moores, A. Panayiotou & C. Xenophontos), pp. 207–16. Nicosia: Geological Survey Department, Ministry of Agriculture and Natural Resources.
- FORNÓS, J. J., CLEMMENSEN, L. B., GÓMEZ-PUJOL, L. & MURRAY, A. S. 2009. Late Pleistocene carbonate aeolianites on Mallorca, Western Mediterranean: a luminescence chronology. *Quaternary Science Reviews* **28**, 2697–709.
- FRÉBOURG, G., HASLER, C.-A., LE GUERN, P. & DAVAUD, E. 2008. Facies characteristics and diversity in carbonate eolianites. *Facies* **54**, 175–91.
- HAKYEMEZ, Y., TURHAN, N., SOŃMEZ, I. & SUŃENGEN, M. 2000. *Kuzey Kıbrıs Türk Cumhuriyeti’ nin Jeolojisi [Geology of the Turkish Republic of Northern Cyprus]*. Ankara: Mineral Research and Exploration Institute of Turkey, Report, 44 pp.
- HANSEN, K. S. 1999. Development of a prograding carbonate wedge during sea level fall: Lower Pleistocene of Rhodes, Greece. *Sedimentology* **46**, 559–76.
- HARRISON, R. W., NEWELL, W. L., BATIHANLI, H., PANAYIDES, I., MCGEEHIN, J. P., MAHAN, S. A., ÖZHÜR, A., TSIOLAKIS, E. & NECDET, M. 2004. Tectonic framework and Late Cenozoic tectonic history of the northern part of Cyprus: implications for earthquake hazards and regional tectonics. *Journal of Asian Earth Sciences* **23**, 191–210.
- HARRISON, R., NEWELL, W., PANAYIDES, I., STONE, B., TSIOLAKIS, E., NECDET, M., BATIHANLI, H., OZHUR, A., LORD, A., BERKSOY, O., ZOMENI, Z. & SCHINDLER, J. S. 2008. *Bedrock Geologic Map of the Greater Lefkosia Area, Cyprus*. U. S. Geological Survey Scientific Investigations Map 3046, scale 1:25 000, 36 pp.
- HEARTY, P. J. & O’LEARY, M. J. 2008. Carbonate eolianites, quartz sands, and Quaternary sea-level cycles, Western Australia: a chronostratigraphic approach. *Quaternary Geochronology* **3**, 26–55.
- HENSON, F. R. S., BROWNE, R. V. & MCGINTY, J. 1949. A synopsis of the stratigraphy and geological history of Cyprus. *Quarterly Journal of the Geological Society* **105**, 1–41.
- KEMPLER, D. 1998. Eratosthenes seamount: the possible spearhead of incipient continental collision in the Eastern Mediterranean. In *Proceedings of the Ocean Drilling Program, Scientific Results, vol. 160* (eds A. H. F. Robertson, K. Emeis, C. Richter & A. Camerlenghi), pp. 709–21. College Station, Texas.
- KINDLER, P. & MAZZOLINI, D. 2001. Sedimentology and petrography of dredged carbonate sands from Stocking Island (Bahamas). Implications for meteoric diagenesis and aeolianite formation. *Palaeogeography, Palaeoclimatology, Palaeoecology* **175**, 369–79.
- KINNAIRD, T. & ROBERTSON, A. 2013. Tectonic and sedimentary response to subduction and incipient continental collision in southern Cyprus, easternmost

- Mediterranean region. In *Geological Development of Anatolia and the Eastern* (eds A. H. F. Robertson, O. Parlak & Ü. Ünlügenç), pp. 585–614. Geological Society of London, Special Publication no. 372.
- KINNAIRD, T. C., ROBERTSON, A. H. F. & MORRIS, A. 2011. Timing of uplift of the Troodos Massif (Cyprus) constrained by sedimentary and magnetic polarity evidence. *Journal of the Geological Society, London* **168**, 457–70.
- KOLLA, V., BIONDI, P., LONG, B. & FILLON, R. 2000. Sequence stratigraphy and architecture of the Late Pleistocene Lagnappe delta complex, northeast Gulf of Mexico. In *Sedimentary Responses to Forced Regressions* (eds D. Hunt & R. L. Gawthorpe), pp. 291–32. Geological Society of London, Special Publication no. 172.
- KOURAMPAS, A. & ROBERTSON, A. H. F. 2000. Controls on Plio-Quaternary sedimentation within an active forearc region: Messenia Peninsula (SW Peloponnese), S. Greece. In *Proceedings of the Third International Conference on the Geology of the Eastern Mediterranean* (eds I. Panayides, C. Xenophonotos & J. Malpas), pp. 255–85. Nicosia: Geological Survey Department, Ministry of Agriculture and Natural Resources and Environment.
- LORD, A. R., PANAYIDES, E. U. & XENOPHONTOS, C. 2000. A biochronostratigraphical framework for the Late Cretaceous–Recent circum-Troodos sedimentary sequence, Cyprus. In *Proceedings of the Third International Conference on the Geology of the Eastern Mediterranean* (eds I. Panayides, C. Xenophonotos & J. Malpas), pp. 289–97. Nicosia: Geological Survey Department, Ministry of Agriculture and Natural Resources and Environment.
- MARTÍN-ALGARRA, A., MARTÍN-MARTÍN, M., ANDREO, B., JULIÀ, R. & GONZÁLEZ-GÓMEZ, C. 2003. Sedimentary patterns in perched spring travertines near Granada (Spain) as indicators of the paleohydrological and paleoclimatological evolution of a karst massif. *Sedimentary Geology* **161**, 217–28.
- MASSARI, F. & CHIOCCI, F. 2006. Biocalcarene and mixed cool-water prograding bodies of the Mediterranean Pliocene and Pleistocene: architecture, depositional setting and forcing factors. In *Cool-Water Carbonates: Depositional Systems and Palaeoenvironmental Controls* (eds H. M. Pedley & G. Carannante), pp. 95–120. Geological Society of London, Special Publication no. 255.
- MCCALLUM, J. E. & ROBERTSON, A. H. F. 1990. Pulsed uplift of the Troodos Massif—evidence from the Plio-Pleistocene Mesaoria basin. In *Ophiolites: Oceanic Crustal Analogues, Proceedings of the Symposium “Troodos 1987”* (eds J. Malpas, E. M. Moores, A. Panayiotou & C. Xenophonotos), pp. 217–30. Nicosia: Geological Survey Department, Ministry of Agriculture and Natural Resources.
- MCCALLUM, J. E. & ROBERTSON, A. H. F. 1995a. Late Pliocene–early Pleistocene Athalassa Formation, north central Cyprus: carbonate sand bodies in a shallow sea-way between two emerging landmasses. *Terra Nova* **7**, 265–77.
- MCCALLUM, J. E. & ROBERTSON, A. H. F. 1995b. Sedimentology of two fan-delta systems in the Pliocene–Pleistocene of the Mesaoria Basin, Cyprus. *Sedimentary Geology* **98**, 215–44.
- MCCAY, G. & ROBERTSON, A. H. F. 2012. Late Eocene–Neogene sedimentary geology of the Girne (Kyrenia) Range, northern Cyprus: a case history of sedimentation related to progressive and diachronous continental collision. *Sedimentary Geology* **265–266**, 30–55.
- MCCAY, G. & ROBERTSON, A. H. F. 2013. Upper Miocene–Pleistocene deformation of the Girne (Kyrenia) Range and Dar Dere (Ovgos) lineaments, northern Cyprus: role in collision and tectonic escape in the easternmost Mediterranean region. In *Geological Development of Anatolia and the Easternmost Mediterranean Region* (eds A. H. F. Robertson, P. Osman & U. C. Ünlügenç), pp. 421–45. Geological Society of London, Special Publication no. 372.
- MCCAY, G., ROBERTSON, A. H. F., KROON, D., RAFFI, I., ELLAM, R. M. & NECDET, M. 2013. Stratigraphy of Cretaceous to Lower Pliocene sediments in the northern part of Cyprus based on comparative $^{87}\text{Sr}/^{86}\text{Sr}$ isotopic, nannofossil and planktonic foraminiferal dating. *Geological Magazine* **150**, 333–59.
- NALIN, R. & MASSARI, F. 2009. Facies and stratigraphic anatomy of a temperate carbonate sequence (Capo Colonna terrace, Late Pleistocene, Southern Italy). *Journal of Sedimentary Research* **79**, 210–25.
- NECDET, M. & ANIL, M. 2006. The geology and geochemistry of the gypsum deposits in Northern Cyprus. *Geosound (Yerbilimleri)* **48:49**, 11–49.
- PALAMAKUMBURA, R. N. & ROBERTSON, A. H. F. 2016. Pleistocene terrace formation related to surface tectonic uplift: example of the Kyrenia Range lineament in the northern part of Cyprus. *Sedimentary Geology* **339**, 46–67.
- PALAMAKUMBURA, R. N., ROBERTSON, A. H. F., KINNAIRD, T. C. & SANDERSON, D. C. W. 2016a. Sedimentary development and correlation of Late Quaternary terraces in the Kyrenia Range, northern Cyprus, using a combination of sedimentology and optical luminescence data. *International Journal of Earth Sciences (Geologische Rundschau)* **105**, 439–62.
- PALAMAKUMBURA, R. N., ROBERTSON, A. H. F., KINNAIRD, T. C., VAN CALSTERN, P., KROON, D., TAIT, J. 2016b. Quantitative dating of Pleistocene deposits of the Kyrenia Range, northern Cyprus: implications for timings, rates of uplift and driving mechanisms. *Journal of the Geological Society, London*, published online 3 June 2016. doi: [10.1144/jgs2015-130](https://doi.org/10.1144/jgs2015-130).
- PANTAZIS, T. M. 1978. Cyprus evaporites. In *Initial Reports of the Deep Sea Drilling Project, vol. 42, part 2* (eds D. A. Ross, Y. P. Neprochnov, K. J. Hsü, P. Stoffers, P. Supko, E. S. Timonis, S. F. Percival Jr., A. J. Erickson, E. T. Degens, J. M. Hunt, F. T. Manheim, M. Senalp & A. Traverse), pp. 1185–94. Washington: U.S. Government Printing Office.
- PEDLEY, M. & CARANNANTE, G. 2006. Cool-water carbonate ramps: a review. In *Cool-water Carbonates: Depositional Systems and Palaeoenvironmental Controls* (eds H. M. Pedley & G. Carannante), pp. 1–9. Geological Society of London, Special Publication no. 255.
- PEDLEY, M. & GRASSO, M. 2002. Lithofacies modelling and sequence stratigraphy in microtidal cool-water carbonates: a case study from the Pleistocene of Sicily, Italy. *Sedimentology* **49**, 533–53.
- POOLE, A. & ROBERTSON, A. H. F. 1998. Pleistocene fan-glomerate deposition related to uplift of the Troodos Ophiolite, Cyprus. In *Proceedings of the Ocean Drilling Program, Scientific Results, vol. 160* (eds A. H. F. Robertson, K.-C. Emeis, C. Richter & A. Camerlenghi), pp. 545–66. College Station, Texas.
- POOLE, A. J. & ROBERTSON, A. H. F. 2000. Quaternary marine terrace and aeolinites in coastal south and west Cyprus: implications for regional uplift and sea-level

- change. In *Proceedings of the Third International Conference on the Geology of the Eastern Mediterranean* (eds I. Panayides, C. Xenophontos & J. Malpas), pp. 105–23. Nicosia: Geological Survey Department, Ministry of Agriculture and Natural Resources.
- POOLE, A. J., SHIMMIELD, G. B. & ROBERTSON, A. H. F. 1990. Late Quaternary uplift of the Troodos ophiolite, Cyprus: uranium-series dating of Pleistocene coral. *Geology* **18**, 894–7.
- POSAMENTIER, H. W. & MORRIS, W. R. 2000. Aspects of the stratal architecture of forced regressive deposits. In *Sedimentary Responses to Forced Regressions* (eds D. Hunt & R. L. Gawthorpe), pp. 19–46. Geological Society of London, Special Publication no. 172.
- RAMOS, E., CABRERA, L., HAGEMANN, H. W., PICKEL, W. & ZAMARREÑO, I. 2001. Palaeogene lacustrine record in Mallorca (NW Mediterranean, Spain): depositional, palaeogeographic and palaeoclimatic implications for the ancient southeastern Iberian margin. *Palaeogeography, Palaeoclimatology, Palaeoecology* **172**, 1–37.
- ROBERTSON, A. H. F. 1977. Tertiary uplift history of the Troodos massif, Cyprus. *Geological Society of America Bulletin* **12**, 1763–72.
- ROBERTSON, A. H. F. 1990. Tectonic evolution of Cyprus. In *Ophiolites: Oceanic Crustal Analogues, Proceedings of the Symposium "Troodos 1987"* (eds J. Malpas, E. M. Moores, A. Panayiotou & C. Xenophontos), pp. 235–52. Nicosia: Geological Survey Department, Ministry of Agriculture and Natural Resources.
- ROBERTSON, A. H. F. 1998. Tectonic significance of the Eratosthenes Seamount: a continental fragment in the process of collision with a subduction zone in the eastern Mediterranean (Ocean Drilling Program Leg 160). *Tectonophysics* **298**, 63–82.
- ROBERTSON, A. H. F. & DIXON, J. E. 1984. Introduction: aspects of the geological evolution of the Eastern Mediterranean. In *The Geological Evolution of the Eastern Mediterranean* (eds J. E. Dixon & A. H. F. Robertson), pp. 1–74. Geological Society of London, Special Publication no. 17.
- ROBERTSON, A. H. F., EATON, S., FOLLOWS, E. J. & PAYNE, A. S. 1995. Depositional processes and basin analysis of Messinian evaporites in Cyprus. *Terra Nova* **7**, 233–53.
- ROBERTSON, A. H. F. & KINNAIRD, T. C. 2016. Structural development of the central Kyrenia Range (north Cyprus) in its regional setting in the eastern Mediterranean region. *International Journal of Earth Sciences* **105**, 417–37.
- ROBERTSON, A. H. F., MCCAY, G. A., TASLI, K. & YILDIZ, A. 2013. Eocene development of the northerly active continental margin of the Southern Neotethys in the Kyrenia Range, north Cyprus. *Geological Magazine* **151**, 692–731.
- ROBERTSON, A. H. F., PARLAK, O. & USTAÖMER, T. 2012. Overview of the Palaeozoic – Neogene evolution of Neotethys in the Eastern Mediterranean region (southern Turkey, Cyprus, Syria). *Petroleum Geoscience* **18** (2004), 381–404.
- ROBERTSON, A. H. F. & WOODCOCK, N. H. 1986. The role of the Kyrenia Range Lineament, Cyprus, in the geological evolution of the eastern Mediterranean area. In *Major Crustal Lineaments and their Influences on the Geological History of Continental Lithosphere* (eds H. G. Reading, J. Watterson & S. H. White), pp. 141–77. *Philosophical Transactions of the Royal Society A: Mathematical, Physical and Engineering Sciences* **317**.
- SCHILDGEN, T. F., COSENTINO, D., BOOKHAGEN, B., NIEDERMANN, S., YILDIRIM, C., ECHTLER, H., WITTMANN, H. & STRECKER, M. R. 2012. Multi-phased uplift of the southern margin of the Central Anatolian plateau, Turkey: a record of tectonic and upper mantle processes. *Earth and Planetary Science Letters* **317–318**, 85–95.
- SCHIRMER, W., WEBER, J., BACHTADSE, V., BOUDAGHERFADEL, M., HELLER, F., LEHMKUHL, F., PANAYIDES, I. & SCHIRMER, U. 2010. Fluvial stacking due to plate collision and uplift during the Early Pleistocene in Cyprus. *Central European Journal of Geosciences* **2**, 514–23.
- ŞENGÖR, A. M. C., GÖRÜR, N. & SAROĞLU, F. 1985. Strike-slip faulting and related basin formation in zones of tectonic escape: Turkey as a case study. In *Strike-Slip Deformation, Basin Formation and Sedimentation* (eds K. D. Biddle & N. Christie-Blick), pp. 227–64. Society of Economic Paleontologists and Mineralogists, Special Publication no. 17.
- STOCKMAL, G. S. & BEAUMONT, C. 1987. Geodynamic models of convergent margin tectonics: the southern Canadian Cordillera and the Swiss Alps. *Sedimentary Basins and Basin-Forming Mechanisms* **12**, 393–411.
- TROPEANO, M. & SABATO, L. 2000. Response of Plio-Pleistocene mixed bioclastic-lithoclastic temperate-water carbonate systems to forced regressions: the Calcarene di Gravina Formation, Puglia, SE Italy. *Sedimentary Responses to Forced Regressions* (eds D. Hunt & R. L. Gawthorpe), pp. 217–43. Geological Society of London, Special Publication no. 172.
- WEBER, J., SCHIRMER, W., HELLER, F. & BACHTADSE, V. 2011. Magnetostratigraphy of the Apalós Formation (early Pleistocene): evidence for pulsed uplift of Cyprus. *Geochemistry, Geophysics, Geosystems* **12**, Q01Z22, doi: [10.1029/2010GC003193](https://doi.org/10.1029/2010GC003193).
- WEILER, Y. 1970. Mode of occurrence of pelites in the Kythrea Flysch basin (Cyprus). *Journal of Sedimentary Research* **40**, 1255–61.
- WRIGHT, V. P. 1989. Terrestrial stromatolites and laminar calcretes: a review. *Sedimentary Geology* **65**, 1–13.